Tracing nitrogen in volcanic and geothermal volatiles from the Nicaraguan volcanic front

L.J. Elkins [a,*], T.P. Fischer [a], D.R. Hilton [b], Z.D. Sharp [a], S. McKnight [c], J. Walker [d]

[a] *Earth and Planetary Sciences Department, University of New Mexico, Albuquerque, NM 87131, USA*
[b] *Fluids and Volatiles Laboratory, Scripps Institution of Oceanography, University of California San Diego, La Jolla, CA 92093-0244, USA*
[c] *URS Corporation, 221 Main St., Suite 600, San Francisco, CA, USA*
[d] *Department of Geology and Environmental Geosciences, Northern Illinois University, DeKalb, IL 60115, USA*

Abstract

We report new chemical and isotopic data from 26 volcanic and geothermal gases, vapor condensates, and thermal water samples, collected along the Nicaraguan volcanic front. The samples were analyzed for chemical abundances and stable isotope compositions, with a focus on nitrogen abundances and isotope ratios. These data are used to evaluate samples for volatile contributions from magma, air, air-saturated water, and the crust. Samples devoid of crustal contamination (based upon He isotope composition) but slightly contaminated by air or air-saturated water are corrected using N_2/Ar ratios in order to obtain primary magmatic values, composed of contributions from upper mantle and subducted hemipelagic sediment on the down-going plate. Using a mantle endmember with $\delta^{15}N = -5‰$ and $N_2/He = 100$ and a subducted sediment component with $\delta^{15}N = +7‰$ and $N_2/He = 10,500$, the average sediment contribution to Nicaraguan volcanic and geothermal gases was determined to be 71%. Most of the gases were dominated by sediment-derived nitrogen, but gas from Volcán Mombacho, the southernmost sampling location, had a mantle signature (46% from subducted sediment, or 54% from the mantle) and an affinity with mantle-dominated gases discharging from Costa Rica localities to the south. High $CO_2/N_{2\ exc.}$ ratios ($N_{2\ exc.}$ is the N_2 abundance corrected for contributions from air) in the south are similar to those in Costa Rica, and reflect the predominant mantle wedge input, whereas low ratios in the north indicate contribution by altered oceanic crust and/or preferential release of nitrogen over carbon from the subducting slab. Sediment-derived nitrogen fluxes at the Nicaraguan volcanic front, estimated by three methods, are 7.8×10^8 mol N/a from ^{3}He flux, 6.9×10^8 mol/a from SO_2 flux, and 2.1×10^8 and 1.3×10^9 mol/a from CO_2 fluxes calculated from ^{3}He and SO_2, respectively. These flux results are higher than previous estimates for Central America, reflecting the high sediment-derived volatile contribution and the high nitrogen content of geothermal and volcanic gases in Nicaragua. The fluxes are also similar to but higher than estimated hemipelagic nitrogen inputs at the trench, suggesting addition of N from altered oceanic basement is needed to satisfy these flux estimates. The similarity of the calculated input of N via the trench to our calculated outputs suggests that little or none of the subducted nitrogen is being recycled into the deeper mantle, and that it is, instead, returned to the surface via arc volcanism.

1. Introduction

The stable isotope compositions and relative abundances of nitrogen in gases from fumaroles and hot springs record inputs to arc-setting geothermal and volcanic gases by reservoirs such as air, the mantle wedge, and the subducted slab. Despite the overwhelming presence of nitrogen in air, it is still possible to identify contributions from these other reservoirs because each has a distinctive chemical and isotopic nitrogen signature (Peters et al., 1978; Marty, 1995; Giggenbach, 1996; Marty and Humbert, 1997; Fischer et al., 2002; Ozima and Podosek, 2002). Nitrogen is therefore an excellent tracer of arc-related processes, as it is capable of fingerprinting gas sources and quantifying relative contributions to the volatile cycle at subduction

* Corresponding author. Present address: Department of Geology and Geophysics, Woods Hole Oceanographic Institution, Woods Hole, MA 02543, USA.
 E-mail address: lelkins@whoi.edu (L.J. Elkins).

zones (Fischer et al., 2002; Hilton et al., 2002). When this capability is used in combination with carbon and helium abundances and isotope data, it is possible to develop holistic models for volatile behavior in subduction zones (e.g. Hilton et al., 2002).

To better understand the nitrogen cycle in subduction zones, we focus on the Nicaraguan segment of the Central American Volcanic Arc (CAVA), as it represents an end-member case study in its contribution of slab-derived inputs to melt generation at arcs. Nicaragua has the steepest angle of subduction and the greatest overall slab influence on lava composition in Central America (Carr, 1984; Carr et al., 1990; Leeman et al., 1994; Protti et al., 1995); Nicaraguan lavas have the highest cosmogenic, slab-derived ^{10}Be signatures of any volcanic rocks worldwide (Morris et al., 1990; Leeman et al., 1994) and the highest B/La ratios in Central American lavas, suggesting significant slab-derived fluid contributions to the magmas (Carr et al., 1990). The high ^{10}Be (Morris et al., 1990) and high U/La and Ba/Th ratios in Nicaragua (Patino et al., 2000) underscore the importance of the transportation of sediment-derived material from the slab to the volcanic front. Recent work by Eiler et al. (2005) on oxygen isotopes in phenocrysts suggests the influence of a low ^{18}O, solute-rich aqueous fluid produced by dehydration of altered rocks within the Cocos Plate, perhaps serpentinites. This aqueous fluid component dominates the slab flux beneath Nicaragua and is the principal control on the extent of mantle melting.

To date, gas discharges have been examined for helium, carbon, and nitrogen in Guatemala and Costa Rica (Fischer et al., 2002; Hilton et al., 2002; Shaw et al., 2003; Zimmer et al., 2004), and for helium and carbon in Nicaragua (Shaw et al., 2003) and along the entire length of the CAVA (Snyder et al., 2001). Snyder et al. (2003) investigated the sources of nitrogen and methane in geothermal fluids along the Central American Arc. Their work focused on geothermal well fluids and concluded that most of the nitrogen discharging in Nicaragua is crustal in origin, based on high $N_2/^3$He, magmatic ^{3}He/^{4}He ratios, and an inferred relationship between excess nitrogen and an iodine isotopic component that is much older than the subducted sediments. Snyder et al. (2003), however, report nitrogen isotope values for only one locality in Nicaragua (Momotombo geothermal wells). In this communication, we expand this database and investigate the relative abundance and isotopic composition of nitrogen in a number of fumaroles, hot springs, and geothermal wells. We argue that the geochemical evidence of significant slab-derived sediment inputs to arc-derived magmas in Nicaragua makes this location an ideal setting in which to further test the sensitivity of nitrogen as a tracer of subducted volatiles. We present a detailed study of geothermal manifestations along the strike of the Nicaraguan volcanic front with the aim of identifying and characterizing reservoirs that contribute to the volatile flux emitted along volcanic arcs in general, and in Nicaragua in particular.

2. Geologic setting

The CAVA is the result of eastward subduction of the Cocos Plate beneath the Caribbean Plate. The subducting plate comprises 170 m of hemipelagic sediments overlying 400 m of limestones which, in turn, overlie oceanic basalt basement (Von Huene et al., 1980). The crustal basement ranges in age from ~13 to 17 Ma at the trench adjacent to Costa Rica to ~25 to 30 Ma off Nicaragua (Protti et al., 1995). The dip of the slab is steepest off Nicaragua (up to 84°) and this is relatively constant throughout the country despite abrupt changes in the surface orientation of the volcanic front (Protti et al., 1995). Convergence direction is nearly orthogonal to the volcanic front in Nicaragua, with convergence rates currently proceeding at about 90 mm/a (Minster and Jordan, 1978; DeMets et al., 1990; Corti et al., 2005). Crustal thickness is less than 35 km in Nicaragua whereas it is greater in both Guatemala (~50 km) and Costa Rica (42 km; Carr et al., 1990).

Western Nicaraguan volcanic rocks are characterized by high Ba/La, B/La, and ^{10}Be/^{9}Be ratios (Carr et al., 1990; Morris et al., 1990; Leeman and Carr, 1995). These features indicate high degrees of partial melting in the mantle beneath Nicaragua, with addition of fluid mobile elements from the uppermost part of the subducting sediment column. These same ratios are low in Costa Rica and intermediate in eastern Nicaragua, Guatemala, and El Salvador (Carr et al., 1990; Leeman et al., 1994; Patino et al., 2000). A proposed explanation for these observations is that due to the steep subduction angle beneath Nicaragua, volatiles are released into only a small volume of mantle wedge above the slab (Carr et al., 1990). Consequently, the release of fluids generates a high degree of partial melting but an overall small melt volume. In this scenario, the Nicaraguan melts incorporate large amounts of fluids from the uppermost layers of the down-going sediment column, thereby concentrating the cosmogenic ^{10}Be signature. Conversely, the shallow dip of the slab beneath Costa Rica explains the generation of large volumes of small-degree melts and consequent dilution of the recycled beryllium signature (Carr, 1984; Carr et al., 1990). Underplating of the uppermost part of the sediment column beneath the overriding crust also has been proposed to explain low cosmogenic ^{10}Be signatures in Costa Rica lavas (Morris et al., 1990; Leeman et al., 1994). Recent work by Eiler et al. (2005) expands on the model of Carr et al. (1990) and accounts for along-arc variations in δ^{18}O values of olivine phenocrysts by mixing of two slab-derived fluid components with mantle wedge: 1. high δ^{18}O values in Guatemala originate from addition of a water-poor partial sediment melt, and 2. low δ^{18}O values in Nicaragua are the result of dehydration of serpentinized oceanic basement, producing a water-rich fluid. Costa Rican lavas show negligible contribution from the high-δ^{18}O water-poor component, and this may reflect a relatively low subduction flux of hemipelagic sediments beneath this section of the arc (Eiler et al., 2005).

Volatile data from Costa Rica and Guatemala provide strong support for the suggestions outlined above. Nitrogen isotope ratios of +5‰ and relative abundances (e.g. high N_2/He) in Guatemalan volcanic and geothermal gases show a strong hemipelagic sedimentary signature, whereas Costa Rican gases have low N_2/He and isotopically light nitrogen, thus supporting a predominant mantle wedge input for the nitrogen (Fischer et al., 2002; Zimmer et al., 2004). Snyder et al. (2003) report N_2/Ar ratios of geothermal wells and fumaroles ranging from ~100 to >800 (air = 84) for Nicaragua, and significantly lower ratios (~40 to ~100) for Costa Rica. Based on correlations between N_2/Ar and $CH_4/^3He$ ratios as well as ^{129}I ages, these authors argue that the elevated N_2/Ar ratios in Nicaragua gases can be attributed to a significant crustal contribution. In the case of carbon, Shaw et al. (2003) found little variation in the L/S ratio (where L = carbonate-derived subducted carbon and S = organic-rich subducted carbon)

along the strike of the arc from Costa Rica to Nicaragua. However, they calculated a higher (L + S)/M ratio in Nicaragua than in Costa Rica (M = carbon derived from the mantle wedge). This observation was interpreted to be consistent with (a) a high slab-derived fluid input into Nicaraguan magma sources and/or a cooler thermal regime beneath Nicaragua promoting increased efficiency of volatile subduction, and (b) offscraping of the uppermost part of the subducting sediment column beneath Costa Rica.

3. Samples and methods

Gas, water, and vapor condensate samples were collected from seven volcanic centers along the Nicaraguan volcanic front. Sample locations are summarized in Table 1 (also available as Electronic annex) and shown in Fig. 1. The northernmost sampling location was Volcán (V.) Cosegüina, and the southernmost samples were collected from

Table 1
Nicaraguan sample type and location

Location	Sample ID	Symbol[a]	Date	Type[b]		Latitude (°N)	Longitude (°W)	T (°C)
Mombacho								
V. Mombacho	Nic-15/1	MB	1/10/2002	FC	Volc.	11.8343	85.9824	110
V. Mombacho	Nic-15/2	MB	1/10/2002	MF	Volc.	11.8343	85.9824	98.0
V. Mombacho	Nic-16	MB	1/10/2002	FC	Vap.	11.8343	85.9824	110
Masaya								
V. Masaya	Nic-7	MA	1/7/2002	FF	Geoth.	11.9991	86.1506	72.5
Tipitapa	Nic-8	TI	1/8/2002	BF	G + W	12.2030	86.0921	70.3
Tipitapa	Nic-10	TI	1/8/2002	BF	Wat.	12.2030	86.0921	70.3
Xiloá	Nic-1	X	1/4/2002	BF	Geoth.	12.2310	86.3227	71.4
Momotombo								
Ormat power plant	Nic-14	MW	1/9/2002	GF	Geoth.	12.3978	86.5520	300
Ormat power plant	Nic-13	MW	1/9/2002	GF	Geoth.	12.4002	86.5535	290
V. Momotombo	Nic-2	MM	1/5/2002	FC	Volc.	12.4243	86.5388	747
V. Momotombo	Nic-3	MM	1/5/2002	FC	Volc.	12.4243	86.5388	747
V. Momotombo	Nic-4	MM	1/5/2002	FC	Vap.	12.4243	86.5388	747
La Chistata	Nic-6	MG	1/6/2002	WF	Wat.	12.4403	86.6135	47.2
San Francisco Libre	Nic-11	SF	1/8/2002	WF	Wat.	12.4984	86.2811	86.1
San Francisco Libre	Nic-12	SF	1/8/2002	WF	G + W	12.4984	86.2811	86.1
Cerro Negro								
V. Cerro Negro	Nic-22	CN	1/16/2002	FC	Geoth.	12.5069	86.7015	310
V. Cerro Negro	Nic-23	CN	1/16/2002	FC	Geoth.	12.5069	86.7015	310
V. Cerro Negro	Nic-24	CN	1/16/2002	FC	Volc.	12.5069	86.7015	97.7
Telica								
San Jacinto	Nic-17	SJ	1/13/2002	BF	G + W	12.5817	86.7793	86.4
San Jacinto	Nic-18	SJ	1/13/2002	BF	Wat.	12.5817	86.7793	86.4
V. Telica	Nic-26	TE	1/17/2002	WF	Wat.	12.6281	86.8279	72.5
V. Telica	Nic-27	TE	1/17/2002	BF	Geoth.	12.6281	86.8279	72.5
San Cristóbal								
V. San Cristóbal	Nic-20	SC	1/15/2002	FC	Geoth.	12.7020	87.0040	95.6
V. San Cristóbal	Nic-21	SC	1/15/2002	FC	Geoth.	12.7020	87.0040	95.6
Cosegüina								
V. Cosegüina	Nic-28	CO	1/19/2002	WF	Wat.	12.9646	87.4937	42
V. Cosegüina	Nic-29	CO	1/19/2002	WF	G + W	12.9646	87.4937	42

[a] Symbols are used to identify sample locales in figures.
[b] First letter: F, fumarole; M, bubbling mudpot; B, bubbling spring; G, geothermal well; W, water spring; second letter: C, summit crater; F, flank. Geoth., geothermal gas; Volc., volcanic gas; Wat., thermal water; Vap., vapor condensate; G + W, gas plus water, indicating that spring water was allowed to enter the sampling flask in order to collect more gas.
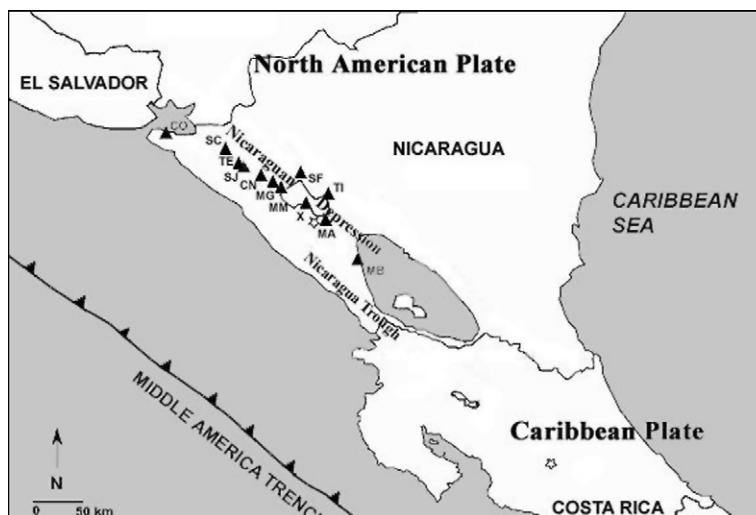
Fig. 1. Map showing locations along the Nicaraguan volcanic front where volcanic gas, geothermal gas, thermal water, and vapor condensate samples were collected in January 2002 for this study. Samples were collected from V. Mombacho, V. Masaya (including locations Tipitapa and Xilóa), V. Momotombo (including geothermal wells at the Ormat power plant, and sampling locations La Chistata and San Francisco Libre), V. Cerro Negro, V. Telica (including San Jacinto), V. San Cristóbal, and V. Coseguïna.

V. Mombacho. The samples from La Chistata (Monte Galán) and San Francisco Libre are associated with V. Momotombo through fault systems, and Tipitapa is likewise associated with V. Masaya.

Gases were collected from bubbling springs and fumaroles in Pyrex flasks using techniques described by Giggenbach and Goguel (1989). At four spring locations characterized by particularly low gas flow rates, spring water was collected along with the gas to facilitate exsolution of the gas from the gas-saturated waters in the evacuated sampling flasks. Thermal waters were collected in six locations. At each of these localities, one untreated water and two filtered waters were collected, and nitric acid was added to one of the filtered water samples. Two vapor condensates were collected from the strongest fumaroles. (For more details on collection methods and sampling localities, see Electronic annex EA-1.)

Gas chemistry was measured in the Volcanic and Hydrothermal Fluids Analysis Laboratory at the University of New Mexico using gas chromatography and wet chemical techniques described by Giggenbach and Goguel (1989). Nitrogen isotope ratios were measured on gas splits using a Finnigan Delta Plus XL stable isotope mass spectrometer with a Finnigan Mat gas bench interface (methods after Fischer et al., 2002; Zimmer et al., 2004). Oxygen and hydrogen isotopes for the waters and vapor condensates were measured using the same mass spectrometer and a high temperature thermal reduction method (Sharp et al., 2001). Water chemistry was measured using atomic absorption spectroscopy (Beaty and Kerber, 1993) and ion chromatography (Smith, 1988; for more details on laboratory methods, see EA-1).

Water content was determined for fumarole gases by the weight difference between each bottle before and after sampling. However, for two fumarole gas samples (Masaya

and Nic-23 from Cerro Negro) weight measurements before and after sampling resulted in inconsistent calculations of water content. For these gases, no water concentrations are reported in Table 2 (also available as Electronic annex). Some samples contained high concentrations of hydrogen (100–199 mmol/mol of dry gas) that interfered with resolution of the helium peak on the gas chromatograph (GC). To resolve He from H_2, we removed H_2 from these samples prior to GC analysis with a heated hydrogen trap (see EA-1), followed by a cold trap to remove the water produced.

Another analytical problem inherent to the use of the GC device is the difficulty of separating the species Ar and O_2 in the separation column. To eliminate this problem, the GC has two separate columns, each with a different carrier gas (Ar and H_2), into which sample gas is simultaneously injected during a run. Helium and H_2 are measured in the Ar carrier gas, and all other species (Ar, N_2, CH_4, and CO in this study) are measured with H_2 as the carrier. To allow for measurement of Ar on the H_2 side without oxygen interference, O_2 must be removed from that column with a heated oxygen trap. However, this trap becomes saturated above an O_2 concentration of about 4.5 wt.% (the equivalent O_2 concentration in mole % depends on the bulk composition of the gas, but it is generally above 15 mmol/mol dry gas), above which excess O_2 is recorded by the detector as Ar. We correct the Ar content of the six affected samples in the data table following the technique described in Zimmer et al. (2004).

4. Results

The abundances of gas species for the 26 Nicaraguan samples in this study are reported together with nitrogen isotope values in Table 2. Table 3 (also available as Electronic annex) gives the oxygen and hydrogen isotopes of

Table 2
Geochemistry results for Nicaraguan gas samples in mmol/mol dry gas

Location	Sample ID	T (°C)	X CO$_2$	X S$_t$	X HCl	X HF	X NH$_3$	X He	X H$_2$	X Ar	X O$_2$	X N$_2$	X CH$_4$	X CO	X H$_2$O[d]	δ^{15}N (‰ vs. air)
Mombacho																
V. Mombacho	Nic-15/1	110	767.6	60.3	15.0	0.11	0.102	0.016	155	0.035	<0.01	2.33	0.02	<0.0003	953.0	0.5 ± 0.8
V. Mombacho	Nic-15/2	98.0	709.9	74.1	25.1	0.8	0.04	0.002	184	0.088	<0.01	5.61	0.19	0.0004		−2.2 ± 0.8
Masaya																
V. Masaya	Nic-7	72.5	41.7	0.23	16.5	0.09	0.05	0.051	0.029	7.9[f]	180	753	<0.25	<0.001		1.2 ± 0.1
Tipitapa	Nic-8	70.3	n.d.[c]	15.1	31.6	0.36	0.08	0.023	0.061	4.6	0.42	285	662.4	0.0014		3.0 ± 0.1
Xiloá	Nic-1	71.4	941.7	9.91	9.00	0.0	0.0086	0.021	4.04	0.25	<0.006	33.9	1.0	<0.0002		4.9 ± 0.6
Momotombo																
Ormat power plant	Nic-14	300	930.0	17.4	7.17	0.06	0.376	0.044	0.94	0.031	<0.002	42.6	1.4	0.002	950.7	2.1 ± 0.1
Ormat power plant	Nic-13	290	881.4	15.7	6.59	0.1	0.9	0.007	5.30	0.29	<0.005	77.0	12.8	<0.004	958.3	5.3 ± 0.1
V. Momotombo	Nic-2	747	675.2	62.3	141	10.24	0.019	0.013	93.8	0.029	<0.007	14.7	<0.006	3.0	962.5	4.9 ± 0.5[e]
V. Momotombo	Nic-3	747	677.0	61.4	136	12.9	0.017	0.006	98.1	0.12	<0.009	12.8	<0.007	1.5	955.0	6.9 ± 0.5[e]
San Francisco Libre	Nic-12	86.1	402.5	187	302	6.3	4.11	<0.056	0.99	1.56[f]	14.6	77.7	2.8	<0.004		−2.3 ± 0.2
Cerro Negro																
V. Cerro Negro	Nic-22	310	n.d.	2.02	22.2	0.17	0.17	<0.10	0.12	7.2	181[f]	787	<0.17	<0.006	974.3	−0.6 ± 0.3
V. Cerro Negro	Nic-23	310	50.2	1.84	23.3	0.17	0.20	<0.060	0.2	6.7	166[f]	751	<0.10	<0.07		0.4 ± 0.2
V. Cerro Negro	Nic-24	97.7	742.0	43.5	4.08	0.73	0.02	0.026	0.1	0.63	8.02	201	<0.01	0.064	922.6	4.9 ± 0.1
Telica																
San Jacinto	Nic-17	86.4	262.8	1.37	35.4	0.24	0.078	<0.025[b]	9.24	4.7[f]	111	572	2.9	<0.002		3.2 ± 0.1
V. Telica	Nic-27	72.5	839.4	3.04	2.15	0.05	0.078	0.016	0.04	0.18	<0.04	155	0.13	<0.001		2.3 ± 0.1
San Cristóbal																
V. San Cristóbal	Nic-20	95.6	863.1	0.55	14.2	0.14	0.02	0.005	0.105	1.2	0.29	120	<0.006	0.0002	972.0	−0.5 ± 0.1
V. San Cristóbal	Nic-21	95.6	839.8	0.77	16.5	0.11	0.06	0.007	0.045	1.5	0.63	141	0.01	<0.0003	984.1	0.1 ± 0.2
Cosegüina																
V. Cosegüina	Nic-29	42.0	n.d.	64.0	735	2.6	1.02	0.19	0.164	3.0	47.6[f]	144	<2.2	<0.002		−1.7 ± 0.2
Air[a]																
			0.33					0.052	0.01	9.3	209	781	0.02			0.0

[a] Air composition from Lide (1990).
[b] '<' indicates that the number shown is the detection limit for the technique used.
[c] 'n.d.' indicates no value detected, detection limit unknown.
[d] Water fraction in mmol/mol for total gas is included for fumarole and well samples only. Not shown for springs because of liquid–vapor partitioning.
[e] Momotombo fumarole δ^{15}N data from samples collected by T. Fischer in March 2003 and measured in Y. Sano's laboratory (also by T. Fischer) at the Ocean Research Institute University of Tokyo.
[f] Ar concentrations corrected using method of Zimmer et al. (2004).

Table 3
Geochemistry results for Nicaraguan thermal waters and vapor condensates

Location	Sample ID	Date	T (°C)	pH-field	pH-lab	Stable isotopes (‰ vs. SMOW)		Cations (mg/L)															Carbonate (mg/L)[b]	
						$\delta^{18}O$	δD	K	Na	Fe	Mn	Ca	Mg	Si	Li	F[a]	Cl[a]	NO$_2$	Br[a]	NO$_3$[a]	PO$_4$	SO$_4$	CO$_3$	HCO$_3$
Thermal waters																								
Masaya																								
Tipitapa	Nic-10	1/8/2002	70.3	8.0	8.49	-5.0 ± 0.3	-44.9 ± 0.4	11.2	292	<0.1	0.04	32.0	0.20	63	0.266	5.40	214.9	<10	<2.0	<10	3.7	146.4	5.9	140
Momotombo																								
La Chistata	Nic-6	1/6/2002	47.2	7.0	8.27	-7.5 ± 0.2	-51.1 ± 0.4	30.5	167	<0.1	0.005	93.0	67.3	70	0.165	0.25	166.7	<1.0	<0.2	2.0	<0.2	225.6	n.d.	360
San Francisco Libre	Nic-11	1/8/2002	86.1	7.0	7.60	-8.0 ± 0.1	-50.7 ± 0.4	3.4	112	<0.1	0.01	136.7	<0.1	28	0.102	1.28	77.5	<1.0	0.2	0.1	<0.2	637.8	n.d.	26
Telica																								
San Jacinto	Nic-18	1/13/2002	94		3.06	2.3 ± 0.3	-17.6 ± 1.8	9	23	13.3	1.5	85.5	24.7	107	<0.03	<100	<100	20.0	<20	<100	48.0	737.0	n.d.	n.d.
V. Telica	Nic-26	1/17/2002	72.5	3.0	2.87	-7.5 ± 0.05	-49.1 ± 0.6	5.4	36	45.4	0.4	37.5	9.60	70	<0.03	<10	3.9	<10	<1.8	<10	<0.2	186.5	n.d.	n.d.
Coseguina																								
V. Coseguina	Nic-28	1/19/2002	42	6.5	8.18	-7.7 ± 0.2	-50.0 ± 1.0	16.8	400	0.1	0.005	95.5	27.2	51.5	0.128	2.20	265.5	<10	2.0	<1.4	<2.0	178.6	n.d.	194
Vapor condensates																								
Mombacho	Nic-16/1	1/10/2002	110.4			0.5 ± 0.2	-18.6 ± 0.3																	
Momotombo	Nic-4	1/5/2002	747			2.8 ± 0.4	-10.7 ± 1.4																	

[a] For some analyses detection limits are extremely high because large dilutions were necessary for ion chromatographic analysis.
[b] Carbonate and bicarbonate concentrations could not be measured in samples with low pH.

thermal waters and vapor condensates in addition to the major cation chemistry.

4.1. Reactive gases

Water represents the most abundant species in the gas samples, with abundances ranging from 92.2% (Cerro Negro) to 98.4% of the total gas (San Cristóbal). CO_2 is the second most abundant species in most samples and is most concentrated in a Momotombo geothermal well (Nic-14) at 930 mmol/mol dry gas. Most of the Nicaraguan gas samples have low total sulfur (S_t) concentrations (average of 18 samples is 35.4 mmol/mol dry gas). Hydrogen chloride, HF, and NH_3 occur in low concentrations, with the exception of gases from Momotombo (up to 141 mmol/mol HCl) and samples that include spring water.

The results for samples for which spring water was deliberately taken into the sampling flasks (Punta Huete, Tipitapa, San Jacinto, and Cosegüina) are reported for the combined composition of spring water + gas. Thermal water chemistry for these four sample locations, as well as two other thermal waters from Nicaragua, is reported in Table 3 for comparison. These gases display elevated concentrations of those constituents that commonly partition into an aqueous phase, such as HCl and HF.

4.2. Non-reactive gases and CO_2

Under the assumption that Ar in gas emissions is predominantly air-derived (Giggenbach, 1995), we use N_2/Ar ratios to monitor contamination by air and air-saturated water (asw) using the following equation (Fischer et al., 1998):

$$[N_{2\ exc.}] = [N_2] - (N_2/Ar)_{air\ or\ asw} \times [Ar] \qquad (1)$$

where brackets indicate abundances, and $(N_2/Ar)_{air\ or\ asw}$ is the N_2/Ar ratio of air (84) or air-saturated water (40). The criterion we use to ascertain whether a sample is contaminated with air or asw is the He/Ne ratio, which has been measured on samples collected simultaneously with the present sample suite (Shaw et al., 2003). If a sample has a low air-normalized $^4He/^{20}Ne$ ratio ($X = (^4He/^{20}Ne)_{sample}/(^4He/^{20}Ne)_{air} < 20$; see Shaw et al., 2003), its chemistry is corrected using Eq. (1) and the N_2/Ar value in air. Samples with $X > 20$ are corrected using the N_2/Ar value in asw. The excess nitrogen ($N_{2\ exc.}$) remaining after the correction is used to calculate $N_{2\ exc.}/Ar$ and $N_{2\ exc.}/He$ ratios (Table 4).

Gas discharges are categorized as "arc-type" or "mantle wedge" using $N_{2\ exc.}$, He, and Ar relative abundances. Arc-type samples are characterized by N_2/Ar ratios that exceed the air value (approximately 84) and have N_2/He ratios >1000. Mantle wedge samples have N_2/Ar ratios less than the air value and N_2/He ratios <1000 (Giggenbach, 1996). Based on $N_{2\ exc.}/He$ ratios, samples from Momotombo, Momotombo geothermal wells, Mombacho (Nic-15/2), Masaya, Tipitapa, Telica, Cerro Negro, Xiloá, San Cristóbal, and San Jacinto are "arc-type" gases, whereas

samples from Mombacho (Nic-15/1), Cosegüina, and San Francisco Libre are "mantle wedge" gases. Samples from Mombacho (Nic-15/2) and Tipitapa, however, have low N_2/Ar for arc-type gases; see Section 5.1 for further discussion of these ratios. For further details about gas classification using reactive gases, see the Appendix, Electronic annex EA-5.

The low N_2 contents of mantle wedge gases result in high $CO_2/N_{2\ exc.}$ ratios compared to arc-type gases. The sample from Mombacho, for example, has a $CO_2/N_{2\ exc.}$ ratio of ~600, while arc-type samples display ratios <50. The average $CO_2/N_{2\ exc.}$ ratio from the most robust Nicaraguan gases (see Section 5.1) is 137.5; with the exception of Mombacho (average 595) the mean $CO_2/N_{2\ exc.}$ ratio is 23.0. For comparison, Fischer et al. (1998) calculated a parental $CO_2/N_{2\ exc.}$ ratio of about 80 for gases from Kudryavy, a subduction zone volcano, and Zimmer et al. (2004) measured a $CO_2/N_{2\ exc.}$ ratio of 943 at Poás Volcano in Costa Rica and an average value of 823 for all of Costa Rica.

4.3. Nitrogen isotopic compositions of gases

Nicaraguan gases span nitrogen isotope values from −2.3 to +6.9‰ vs. air. All samples fall between values postulated for reservoirs likely to contribute to arc-related systems: mantle wedge ($\delta^{15}N$ ~–5‰ (Marty and Humbert, 1997) or ~–12‰ (Mohapatra and Murty, 2004)) and hemipelagic sedimentary material ($\delta^{15}N$ ~+7‰; Peters et al., 1978; Sadofsky and Bebout, 2004). Gases containing the highest nitrogen isotope ratios were collected from Momotombo crater (+4.9 and +6.9‰), Xiloá (+4.9‰), a Momotombo geothermal well (+5.3‰), and Cerro Negro (+4.9‰), and the lowest values were measured in gases from San Francisco Libre in the Momotombo complex (−2.3‰), Mombacho (−2.2‰), and Cosegüina (−1.7‰). All samples contain some air-derived nitrogen ($\delta^{15}N = 0$‰) and are corrected to more extreme values (see Section 5.2).

4.4. Water chemistry and isotopic compositions

The chemical compositions of six Nicaraguan thermal waters are reported in Table 3 (EA-4). The water compositions fall into all three thermal water classifications, as defined by Giggenbach et al. (1990) and Chiodini et al. (1996): neutral chloride–sulfate, neutral bicarbonate, and acid neutral sulfate (see EA-5 for more details).

Oxygen and hydrogen isotope results for thermal waters and vapor condensates are shown in Table 3 and Fig. 2. The waters from San Francisco Libre, Cosegüina, Telica, and La Chistata (Monte Galán) cluster near the meteoric water line (Craig, 1961). The Momotombo vapor condensate is the farthest from the meteoric water line, with $\delta^{18}O = +2.8 \pm 0.4$‰ and $\delta D = -10.7 \pm 1.4$‰. The samples from Tipitapa and San Jacinto lie near a linear trend that connects the meteoric water line (from near the clustered samples) to the Momotombo vapor condensate (slope = 3.64 and $r^2 = 0.984$). This trend could reveal mix-

Table 4
Ratios, calculations, and companion data used to evaluate data integrity

Location	Sample ID	N_2/Ar	N_2/He	$N_{2\ exc.}$	$N_{2\ exc.}/He^*$	CO_2 (mmol/mol)	$CO_2/N_{2\ exc.}$	$\delta^{15}N$ (‰)	X^a	$CO_2/^3He^a$	$\delta^{13}C$ (‰)[a]	$^3He/^4He$ $(R_A)^a$
Mombacho												
V. Mombacho	Nic-15/1	66.0[c]	144.5	0.9[asw]	56.9	767.6	852.9	0.51[c]	735.2	1.78×10^{10}	−3.6	7.59 ± 0.1
V. Mombacho	Nic-15/2	64.1[c]	3277.5	2.1[asw]	1231.5	709.9	338.0	**-2.19**	493.3	1.83×10^{10}	−2.7	6.86 ± 0.05
					644.2	**738.8**	**595.5**		**614.2**		**-3.2**	**7.23**
Masaya												
V. Masaya	Nic-7	95.7	14745	99.7[air]	1953.0	41.7[c]	0.4	1.21	6.4[c]	2.26×10^{10}	−1.5	1.98 ± 0.02^d
Tipitapa	Nic-8	61.9[c]	12645	101.0[asw]	4477.1	n.d.[c]		3.01	189.7	5.93×10^{8d}	−2.1	2.99 ± 0.06^d
Xiloá	Nic-1	133.9	1617.7	23.8[asw]	**1134.2**	**941.7**	**39.6**	**4.88**	**529.1**	1.44×10^{10}	**-2.5**	$\mathbf{7.14 \pm 0.11}$
Momotombo												
Ormat power plant	Nic-14	1384	9993.5	41.4[asw]	10340.0	930.0	22.5	2.11	637.1	3.63×10^{10}	−2.6	6.86 ± 0.1
Ormat power plant	Nic-13	265.5	10807	65.4[asw]	9342.9	881.4	13.5	5.29	430.4	3.12×10^{10}	−1.3	6.35 ± 0.1^d
V. Momotombo	Nic-2	503.4	1134.0	13.6[asw]	1043.9	675.2	49.6	4.90	864.1	2.74×10^{10}	−2.6	6.99 ± 0.07
V. Momotombo	Nic-3	107.3	2260.0	8.0[asw]	1417.6	677.0	84.6	6.90	864.1	2.74×10^{10}	−2.6	6.99 ± 0.07
San Francisco Libre	Nic-12	48.6[c]	1328.2[b]	13.7[asw]	244.6[b]	402.5	29.4	−2.33	176.5	2.86×10^{8d}	−6.2[d]	1.83 ± 0.03^d
					4000.7	**669.8**	**45.5**	**2.2**	**559.2**		**−3.8**	**5.23**
Cerro Negro												
V. Cerro Negro	Nic-22	109.3	7941.5[b]	182.5[air]	1841.1[b]	n.d.[c]		−0.56[c]	2.5[c]	7.40×10^{9d}	−3.2	1.26 ± 0.02^d
V. Cerro Negro	Nic-23	111.3	12686[b]	184.1[air]	3110.2[b]	50.2[c]	0.1	0.36[c]	2.9[c]	1.31×10^{10}	−1.8	1.72 ± 0.03^d
V. Cerro Negro	Nic-24	319.6	7631.3	175.8[asw]	**6761.5**	**742.0**	**4.2**	**4.90**	**30.3**	3.14×10^{10}	**-2.3**	$\mathbf{6.99 \pm 0.07}$
Telica												
San Jacinto	Nic-17	121.3	22927[b]	180.5[air]	7237.4[b]	262.8	1.5	3.25	16.3	1.05×10^{10}	−0.55	5.68 ± 0.07
V. Telica	Nic-27	848.2	9399	147.8[asw]	**9237.5**	**839.4**	**5.7**	**2.27**	**44.6**	4.63×10^{11d}	**−3.2**	$\mathbf{7.41 \pm 1.9}$
San Cristóbal												
V. San Cristóbal	Nic-20	101.8	25193[c]	22.2[air]	4644.2	863.1	38.9	−0.52[c]	12.9	2.55×10^{10}	−3	5.74 ± 0.09
V. San Cristóbal	Nic-21	96.6	18768	19.8[air]	2646.2	839.8	42.4	0.07[c]	12.9	2.55×10^{10}	−3	5.74 ± 0.09
Cosegüina												
V. Cosegüina	Nic-29	48.4[c]	741.6	0[air]	0.0	n.d.[c]		−1.74	4.6[c]	2.57×10^{11d}	−11.4[d]	2.96 ± 0.06^d
Corrected Average				**4355.6**	**786.3**	**138.1**	**2.4**		**355.5**		**−3.0**	**6.80**

Average values for each location shown in bold.

[a] $X = (^4He/^{20}Ne)_{sample}/(^4He/^{20}Ne)_{air}$, $CO_2/^3He$, $\delta^{13}C$, $^3He/^4He$ data selected from Shaw et al. (2003). In locations where Shaw et al. (2003) took more than one sample and we sampled only once, an average of those data which they consider the most robust is shown.

[b] He value used is a detection limit, making this ratio a minimum.

[c] Indicates air or asw contamination using criteria described in text.

[d] Indicates crustal contamination using criteria described in text.

[*] $N_{2\ exc.}/He$ ratio calculations explained in text. 'Air' indicates $N_2/Ar = 84$, and 'asw' denotes $N_2/Ar = 40$ in correction.
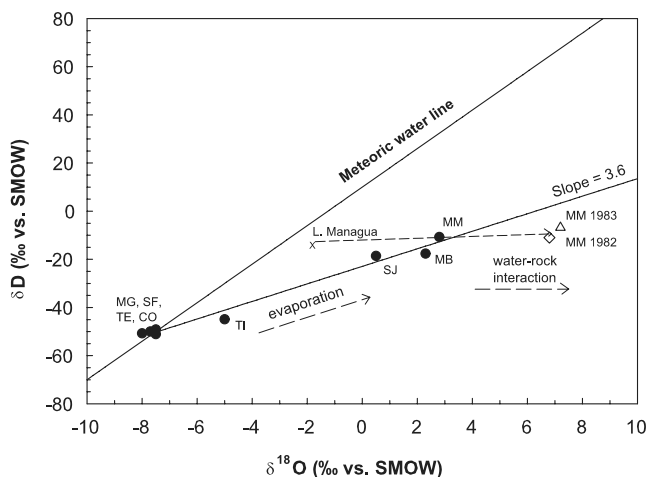
Fig. 2. Plot of δD vs. δ^{18}O showing stable isotopes of Nicaraguan thermal waters (Monte Galan, San Francisco Libre, Telica, Tipitapa, Cosegüina, and San Jacinto) and vapor condensates (Mombacho and Momotombo). Data points form an evaporation trend (thin solid line; slope = 3.6, r^2 = 0.98) departing from the meteoric water line (MWL; Craig, 1961). Momotombo may alternately be derived from water–rock interaction by water from Lake Managua (*X*, dashed line). Also plotted are Momotombo vapor condensate measurements from 1983 (Allard, 1983) to 1982 (Menyailov et al., 1986). Symbols: MG, Monte Galan; SF, San Francisco Libre; TE, Telica; TI, Tipitapa; CO, Cosegüina; SJ, San Jacinto; MB, Mombacho; and MM, Momotombo.

ing between regional meteoric water and a magmatic vapor component. However, mixing is unlikely because extrapolation of the trend to a 'magmatic' δ^{18}O value of +8‰ (Goff and McMurtry, 2000) yields a δD value of +6‰, a value too high for magmatic water (Giggenbach, 1992; Goff and McMurtry, 2000). An alternate, and preferred explanation is that this trend represents evaporation of meteoric waters. The slope of 3.6 agrees with evaporation in geothermal settings (Criss, 1999). Vapor samples from Momotombo reported by Allard (1983) and Menyailov et al. (1986) have similar δD values (−6.8 and −11.0‰, respectively) to the sample measured in this study, but higher δ^{18}O (+7.2 and +6.8‰, respectively). Lake Managua water has a similar δD = −14‰ and a lower δ^{18}O of −1.8‰ (Menyailov et al., 1986; see Fig. 2). It is likely that evaporated lake water has undergone water–rock interaction at Momotombo, increasing the δ^{18}O by progressive oxygen equilibration, but not the δD of the water. The Mombacho vapor condensate lies near the same evaporation line, whereas thermal waters are primarily meteoric. The Mombacho fumarole is characterized by a high water fraction (water/dry gas = 20.3) and nearby acid pools suggest that meteoric waters, affected by evaporation, are entrained in the Mombacho steam.

5. Discussion

5.1. Data integrity

Before drawing on our data to develop models for volatile mass transfer in the Nicaraguan subduction zone, we first identify and eliminate samples which have suffered substantial contamination by air, asw, and/or shallow crustal materials, and are thus unrepresentative of the magma source region. In the following sections, we describe the criteria by which samples have been eliminated from further consideration. Data complementary to those presented here have been published by Shaw et al. (2003); we refer to their He and C results in this section (see Table 4).

Note that sample locales with the highest temperatures and highest gas flow rates were deliberately targeted at each volcanic center. Wherever feasible, samples of different types (spring, fumarole, geothermal well) were collected in an attempt to avoid sampling bias.

5.1.1. Air contamination

There are a number of criteria that can be used to identify samples compromised by air contamination. In the first instance, samples with He contents below detection limits (e.g. San Jacinto, San Francisco Libre, and Nic-22 and -23 from Cerro Negro) and high Ar contents (>1.5 mmol/mol dry gas) that result in He/Ar ratios <0.036 are indicative of samples severely contaminated by air (air He/Ar = 0.00056).

High oxygen contents are also diagnostic of air contamination. Samples from San Francisco Libre, Masaya, San Jacinto, Nic-22 and Nic-23 from Cerro Negro, and Cosegüina have O$_2$ concentrations two to three orders of magnitude greater than other samples. The samples from Masaya and Cerro Negro also contain an order of magnitude less CO$_2$ than most of the other samples. The ^{3}He/^{4}He ratios of these two samples approach the air value of 1 R_A (Shaw et al., 2003). Samples from Masaya, Cerro Negro (Nic-22 and Nic-23) and Cosegüina have *X* values (where $X = (^4He/^{20}Ne)_{sample}/(^4He/^{20}Ne)_{air}$) that are one to two orders of magnitude lower than all other samples, indicating that they are also overwhelmed by air. In summary, the following samples have too much air contamination to be representative of the magmatic source: San Francisco Libre, Masaya, San Jacinto, Nic-22 and Nic-23 from Cerro Negro, and Cosegüina.

5.1.2. Crustal contamination

We consider a gas contaminated by crustal material and unrepresentative of the magma if 15% of crustal He (with ^{3}He/^{4}He = 0.01 R_A) has been added to uncontaminated, magmatic He with an upper mantle isotopic signature (^{3}He/^{4}He = 8 R_A), mixing to produce, upon exsolution and degassing, a gas with a ^{3}He/^{4}He ratio of 6.8 R_A. The samples from Tipitapa, Masaya, San Francisco Libre, Cosegüina, and one geothermal well at Momotombo (Nic-13) have ^{3}He/^{4}He ratios that lie below this value, indicating significant addition of crustal ^{4}He to the gases. The worldwide arc volatile average CO$_2$/^{3}He ratio is ∼1.5 × 10^{10} (Hilton et al., 2002). The samples from San Francisco Libre and Tipitapa have ratios that are two orders of magnitude lower, whereas samples from Telica

and Coseg̈uina have ratios that are an order of magnitude higher than this value, indicative of CO_2 loss or addition in the crust (Shaw et al., 2003). The nitrogen and helium abundances and isotopes of Telica, however, are not significantly different from mantle (e.g. $\delta^{15}N$ distinct from Air and $^3He/^4He$ within error of the upper mantle average of 8 R_A), suggesting that this sample may have been modified with respect to C but not N or He. We consider all other samples listed above sufficiently contaminated by crustal volatiles to exclude them from further interpretation regarding mantle volatile compositions.

The efficiency of nitrogen release from crustal sediments is a temperature-dependent process (Mariner et al., 2003; Snyder et al., 2003). Snyder et al. (2003) suggested that the high nitrogen content of Momotombo well gases reflects contribution from a sedimentary basin characterized by nitrogen with positive $\delta^{15}N$ values, mantle $^3He/^4He$ ratios, and high heat flow. They calculated equilibration temperatures that were 60 and 150 °C higher than measured well temperatures, and they ascribed these differences to the non-equilibrium addition of carbon from crustal methane, and not to prior equilibration of the gas at a higher temperature. Likewise, Mariner et al. (2003) suggested that, in the Cascade volcanoes in the western US, nitrogen addition to subsurface gases occurs in sedimentary units at a temperature between 120 and 140 °C due to the process of albitization. In Fig. 3 we test for systematic, temperature-dependent crustal contamination that affects nitrogen abundances and isotopes. We plot temperature (both measured discharge temperatures and calculated equilibration temperatures) for the gases vs. (a) $N_{2\ exc.}$ and (b) methane. Equilibration temperatures are calculated subsurface tem-

Fig. 3. Discharge and calculated equilibration temperatures vs. CH_4 (upper) and $N_{2\ exc.}$ (lower plot). The general lack of correlations between T and $N_{2\ exc.}$, T and CH_4, or $N_{2\ exc.}$ and CH_4 reveals that the nitrogen in Nicaraguan volcanic and geothermal gases is not affected by temperature-dependent crustal contamination. Temperature calculation methods are shown in Table 5.

peratures at which different groups of gas species would have equilibrated to their measured relative concentrations based entirely on thermodynamic considerations (see Table 5 for details). There is no systematic correlation of excess nitrogen with temperature for our Nicaraguan samples (Fig. 3). The lack of correlation between equilibration temperatures and nitrogen excess indicates that the excess nitrogen is not derived from the shallow crustal release of sedimentary nitrogen. Additionally, if the N in the gases came from the crust, we would expect higher CH_4 contents (believed to be of crustal origin in some hydrothermal systems; Taran et al., 1998) to accompany higher $N_{2\ exc.}$ values. Methane and $N_{2\ exc.}$ do not correlate (not shown) except in samples from Tipitapa, San Francisco Libre, Coseg̈uina, and one Momotombo geothermal well (Nic-13). This observation supports the conclusion that most localities sample N originating predominantly from magmatic processes and not from the overlying crustal sediments, suggesting that the ultimate origin of $N_{2\ exc.}$ must be the mantle wedge or subducted sediments. Tipitapa, San Francisco Libre, Coseg̈uina, and Nic-13 have experienced some crustal contamination, and are excluded from further consideration.

Shaw et al. (2003) suggested that the older geothermal well at Momotombo (Nic-13), which had been producing for 2 years at the time of sampling, may have experienced some contamination as a result of air addition by injection wells and/or groundwater. This was in contrast to a 2-month-old well (sample Nic-14 in this study), whose gas chemistry closely resembles that of the nearby summit fumarole (Table 2). Our data corroborate this suggestion; Nic-13 has a high N_2/He ratio (10,803), a low He/Ar (0.03) ratio, and, as observed above, high CH_4 concentrations and low $^3He/^4He$. Thus, while geothermal well chemistry may be progressively modified with time, other types of samples (e.g. fumaroles) may not be subject to the same type of contamination. Our diverse data set allows us to critically assess the extent to which each sampling method lends itself to modification following magmatic degassing.

5.1.3. Discrepancy between samples collected at the same locality

The two samples from Mombacho have different chemistries and isotopic compositions, and their $\delta^{15}N$ values are particularly disparate (+0.5 and −2.2‰). The samples were collected at different locations, but in close proximity, and on the same day. One sample (Nic-15/1) was collected at a fumarole and the other (Nic-15/2) at a nearby vigorously bubbling spring. The different $\delta^{15}N$ values are not easily attributable to a difference in sample type (fumarole vs. spring), and the gas chemistry of sample Nic-15/1 does not support air contamination during sampling. Instead, we suspect that the nitrogen isotopes in Nic-15/1 have been shifted towards 0‰ due to air contam-

Table 5
Discharge and calculated equilibration temperatures for Nicaraguan gas samples

Location	Sample ID	$T_{discharge}$	Volcanic gases[b]		Geothermal gases[a] T (°C)
			T_c (°C)	T_{meth} (°C)	
Mombacho					
V. Mombacho	Nic-15/1	110.4			285
V. Mombacho	Nic-15/2	98	180	405	270
Masaya					
Xiloá	Nic-1	71.4			200
Momotombo					
Ormat power plant	Nic-14	300			280
Ormat power plant	Nic-13	290.3			85
V. Momotombo	Nic-2	747	>725	>590	
V. Momotombo	Nic-3	747	>645	>580	
Cerro Negro					
V. Cerro Negro	Nic-24	97.7	>395	>565	130
Telica					
San Jacinto	Nic-17	86.4			160
V. Telica	Nic-27	72.5			70
San Cristóbal					
V. San Cristóbal	Nic-20	95.6			80
V. San Cristóbal	Nic-21	95.6			60

[a] D'Amore and Panichi (1980) derived an empirical equation that calculates equilibration temperatures for geothermal gases as a function of partial pressures of different gas species

$$T(°C) = 24,775/(\alpha + \beta + 36.05) - 273.15$$

where $\alpha = 2\log(X_{CH_4}/X_{CO_2}) - 6\log(X_{H_2}/X_{CO_2}) - 3\log(X_{H_2S}/X_{CO_2})$

$$\beta = 7\log(X_{CO_2})$$

and (X_i) is the molar fraction of the gas species i.

[b] Giggenbach et al. (1990) derived an equation for calculating equilibration temperatures of volcanic gases

$$T_c = 14,173/[\log((X_{CO_2})^3(X_{CH_4})/(X_{CO})^4) + 9.83] - 273.15$$

where T_c is the temperature for the equilibration of carbon species. Giggenbach and Soto (1992) also derived an equation for the equilibration temperature T_{meth}, which uses only methane and carbon dioxide concentrations of volcanic gases

$$T_{meth} = 4625/[\log((X_{CH_4})/(X_{CO_2})) + 10.4] - 273.15.$$

'>' signs reflect the use of detection limits for CH_4 concentrations.

ination in the laboratory. This likely occurred after analysis on the GC and prior to isotope measurement, during the taking of the gas split. Both Mombacho samples probably began with the same nitrogen isotope value of −2.2‰, and the GC analysis results are free of this contamination event. Thus, only the nitrogen isotope measurement has been compromised. For the following discussion, we therefore assume that Mombacho sample Nic-15/1 has been compromised by air contamination in the laboratory and that the representative $\delta^{15}N$ value for Mombacho is −2.2‰ (Table 4).

In summary, gas samples that are considered contaminated with crust, air, or asw are San Francisco Libre, Masaya, Tipitapa, Nic-13 from the Momotombo geothermal wells, San Jacinto, San Cristóbal, Nic-22 and Nic-23 from Cerro Negro, and Coseg̈uina. These samples are marked in Table 4 with superscript indicating air/asw or crustal contamination, and are eliminated from further consideration.

5.1.4. Fractionation of volatile species during devolatilization, degassing, and low-temperature processes

Before evaluating the importance of different reservoirs on our gas samples with chemical and isotopic ratios, we must consider the effects of fractionation by secondary or contaminating processes on the chemical and isotopic ratios of the gases. Of particular concern are isotopic and elemental fractionation during subducting slab devolatilization, degassing from the magma chamber, and exsolution from a water phase.

Workers such as Bebout (1995), Bebout and Fogel (1992), and Sadofsky and Bebout (2004) have examined the effect of slab devolatilization on the nitrogen isotope ratios of subducted sediments. Their work suggests that isotopic fractionation during forearc metamorphism and devolatilization of subducted sediments results in somewhat higher $\delta^{15}N$ values in the fluids. Although Sadofsky and Bebout (2004) prefer an average subducted sediment $\delta^{15}N$ value of +5.5‰, we consider higher values (+7‰)

when we model subducted sedimentary nitrogen input to geothermal and volcanic gases to account for this possible fractionation.

Magma chamber degassing can fractionate C, N, Ar, and He from each other, such that gases sampled at the surface do not have the same C/N or N/He ratios as the original magma. Open-system degassing is modeled as a Rayleigh fractionation process, where the elemental ratio in the residual melt is a function of the initial ratio in the melt, the fraction of gas remaining in the melt, and the solubility ratio for the two chemical species in question. For example, the following equation describes Rayleigh fractionation for N_2/He ratios:

$$(N_2/He)_{res} = (N_2/He)_i \times F^{(\alpha-1)/\alpha} \qquad (2)$$

where $(N_2/He)_{res}$ is the residual N_2/He ratio, $(N_2/He)_i$ is the initial N_2/He ratio, F is the fraction of gas remaining in the melt, $\alpha = S_{He}/S_{N_2}$, and S is the solubility of the species in subscript. Using solubilities of 5.98×10^{-5} cm^3/g for N_2 and Ar in basalt (Libourel et al., 2003), 6.0×10^{-4} cm^3/g for He (Jambon et al., 1986; Lux, 1987), and 2.55×10^{-4} cm^3/g for CO_2 (Dixon et al., 1995), and by choosing initial N_2/He, He/Ar, and CO_2/He ratios of 10,000, 0.2, and 20,550, respectively, we can calculate degassing trends (Figs. 4 and 5). Fig. 4 shows that N_2/He ratios that plot within the arc-type field could be produced by various extents of degassing of a high N_2/He endmem-
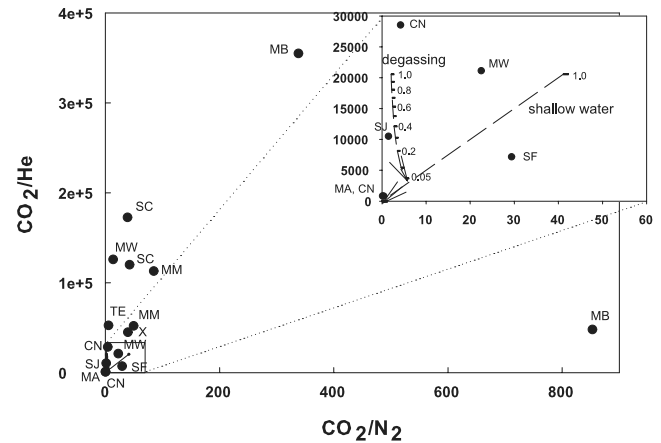
Fig. 5. Diagram of $CO_2/^3$He vs. CO_2/N_2, showing samples from this study and calculated fractionation trends for degassing magma and exsolution from shallow water (calculations explained in Section 5.1.4). Inset shows magnified area of the plot, with calculated trends shown as dashed arrows pointing in the direction of increasing fractionation, and F values as labelled tick marks. Sample CO_2/N_2 values in this diagram are expressed as $CO_2/N_{2, exc}$. Symbols as in Figs. 2 and 4.

ber ($F = 1$ to 0.1) followed by mixing with air or asw. The N_2/He ratios that fall within the mantle-derived field would require volatile discharge from extensively degassed magmas ($F \leqslant 0.001$), again followed by mixing with air or asw. Samples MB, CO, and SF fall into that category. If indeed the N_2/He ratios are the result of various degrees of degassing, samples from extensively degassed magmas (i.e. MB) should also have (a) lower gas fractions or higher H_2O contents due to a higher contribution of meteoric water, and (b) lower ^{3}He/^{4}He ratios due to higher susceptibility to contamination by crustal ^{4}He (Hilton et al., 1993) than samples from less degassed magmas (i.e. MW, MM). Neither is the case, as both MM and MB have almost identical H_2O contents (Table 2) and δD and δ^{18}O values (Fig. 2), and ^{3}He/^{4}He values range from 7.6 R_A for MB to 6.8 R_A for MW (Table 4). We therefore consider it unlikely that the observed variations in N_2–He–Ar systematics are the result of elemental fractionation due to magma degassing. Evidence against N isotope fractionation during magma degassing comes from a suite of MORB glasses(Marty and Dauphas, 2003) and from olivine separates and gas sample pairs, which show that δ^{15}N values are similar between crystallized olivine and gas emissions at a given locality (Fischer et al., 2005).

Similar calculations involving CO_2 show that the CO_2/He and CO_2/N_2 ratios (Fig. 5) are unlikely to be produced by degassing magma. CO_2/He ratios decrease with increased degassing, and CO_2/N_2 ratios increase slightly after extensive degassing. Only the sample SJ plots near this calculated trend, indicating that this sample alone may have experienced some fractionation during degassing of the magma.

Elemental fractionation during exsolution of gases from a shallow water phase is modeled in similar fashion (for Henry's constants of gases in water see Ballentine et al.,
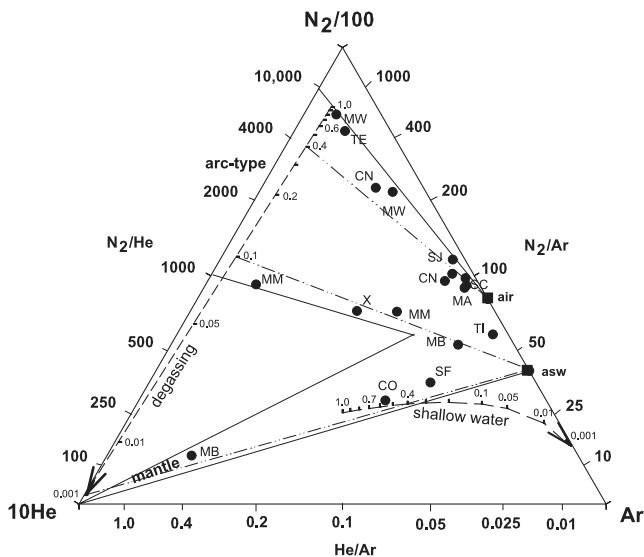
Fig. 4. Triangular plot of N_2, He, and Ar for the Nicaraguan gases. Air, air-saturated water (asw), mantle wedge gases, and arc-type gases are all marked on the diagram as discussed in the text. Calculated fractionation trends for degassing magma and exsolution from shallow water (see Section 5.1.4 for calculations) are shown as dashed lines with arrows pointing in the direction of progressive fractionation (decreasing F, the fraction of gas remaining in the melt or water), and labelled tick marks show calculated values for F. Dash-dot lines represent examples of mixing trends between air or asw and variably degassed magmatic gas. Symbols after Fig. 2, with MA, Masaya; X, Xiloá; MW, Momotombo geothermal wells; SF, San Francisco Libre; CN, Cerro Negro; and SC, San Cristóbal.

2002 and Crovetto, 1996). Because the solubility of $Ar > N_2 > He$ in water, gas exsolution will result in an increase in N_2/He and a decrease in He/Ar ratios. Therefore, degassing of air-saturated water cannot produce the observed N–He–Ar abundance systematics (fractionation due to degassing of water is most significant at temperatures below boiling and we consider bubbling spring samples only). For example, degassing of water with initial N_2/He (500) and He/Ar (0.1), i.e. representing a mixture of mantle-derived gas and asw, would closely approximate the trend for mixing with air-saturated water (Fig. 4). Although some elemental fractionation due to gas exsolution probably occurs, the dominant process likely is mixing of magmatic volatiles with air or asw, which also best explains the N-isotope systematics (see Sections 5.1.1, 5.1.2, 5.2). Similar calculations for CO_2, N_2, and He demonstrate that, because CO_2 is more soluble in water than N_2 or He, CO_2/N_2 and CO_2/He ratios decrease rapidly with degassing from shallow, low temperature water (Fig. 5). Only samples we have already determined to be contaminated by air, asw, or crust (MA, Nic-22 and -23 from CN, CO, and TI; see Sections 5.1.1, 5.1.2) can be explained by this process.

5.2. Gas provenance: resolution into endmembers

Our stringent criteria for sample robustness account for contamination by air, asw, and crustal materials and processes; sample discrepancies; and fractionation during devolatilization, degassing, and shallow crustal interactions (see Section 5.1). We are confident that the isotopic and chemical ratios of the remaining gas samples reflect the compositions and relative contributions of volatile sources in the zone of magma generation beneath the Nicaraguan volcanic front. Here, we attempt to model those contributions.

Giggenbach (1992, 1996) and Fischer et al. (1998) note that volcanic gases from mid-ocean ridges (MOR) and hotspot regions cluster closely near the He apex of a N_2–He–Ar triangular diagram (Fig. 4). Gases from continental settings also plot near the He apex due to addition of crustally derived ^{4}He. Giggenbach (1996) pointed out that gases from convergent margins have higher N_2/He ratios than those from other volcanic areas, plotting near the part of the diagram marked "arc-type" in Fig. 4. He suggested that this is due to variable addition of volatiles from subducted marine sediments to magmas generated in the mantle wedge. He quantified this difference by observing that gases from non-arc regions have N_2/He ratios between 10 and 200, while ratios in arc settings range from 1000 to 10,000. These findings were substantiated by Marty and Zimmermann (1999) who measured a global average MORB N_2/Ar ratio of 124 ± 40. In contrast, marine sediments heated in vacuum produce a range in N_2/Ar ratios between 150 and 21,000 (Matsuo et al., 1978). In a study of volcanic and geothermal gases from Japan, Kita et al. (1993) found high N_2/Ar values in the northeast part of

Japan but lower values in the southwest. They attributed this pattern to the addition of subducted material to the gases in the northeast. These studies reinforce the conclusion that mantle wedge gases have low N_2/He and N_2/Ar, and arc-type gases are characterized by higher N_2/He and N_2/Ar ratios.

The major reservoirs contributing nitrogen to geothermal and volcanic gases in subduction zones are the atmosphere, upper mantle, and subducted hemipelagic sediments (Kita et al., 1993; Sano et al., 2001; Fischer et al., 2002). We use endmember δ^{15}N values for these components of 0‰ (Ozima and Podosek, 2002), -5 ± 2‰ (Marty, 1995; Cartigny et al., 1998; Sano et al., 1998; Marty and Zimmermann, 1999; Sano et al., 2001), and $+7 \pm 4$‰ (Peters et al., 1978; Bebout and Fogel, 1992; Boyd and Pillinger, 1994; Bebout, 1995; Kienast, 2000; Sadofsky and Bebout, 2004; Li and Bebout, 2005) for atmosphere, upper mantle, and subducted hemipelagic sediments, respectively. An additional potential contributor of nitrogen to arc gases is the subducted altered oceanic crust; its δ^{15}N value, however, is currently poorly constrained but may be as low as -2.9‰ (Li et al., 2003). Note that while Sadofsky and Bebout (2004) challenge the use of δ^{15}N $= +7$‰ for subducted sediments, preferring an average value of $+5.5$‰, they state that $+7$‰ is within the range of realistic values due to the possibility of fractionation during forearc metamorphism. We prefer the higher value because samples in both Guatemala and Nicaragua have δ^{15}N higher than $+5.5$‰, making $+7$‰ a more realistic endmember. The N_2/He ratio in air is 1.49×10^5 (Ozima and Podosek, 2002). In marine sediments N_2/He ratios range from 75 to 1.05×10^4, based on the full range of N_2/Ar measurements in marine sediments (Matsuo et al., 1978) and a radiogenic production ^{4}He/^{40}Ar ratio of 2 (Ozima and Podosek, 2002); we use the maximum N_2/He value for our subducted sediment component because it represents the most extreme mixing endmember. The N_2/He ratio in the upper mantle, inferred from MORB glasses, falls within a range of 124 ± 40 (Marty and Zimmermann, 1999).

We use the three-component model of Sano et al. (2001) to approximate the fraction of each endmember contributing to the total nitrogen in the gas discharges

$$(\delta^{15}N)_{obs} = (\delta^{15}N)_A f_A + (\delta^{15}N)_M f_M + (\delta^{15}N)_S f_S \qquad (3)$$

$$1/(N_2/He)_{obs} = f_A/(N_2/He)_A + f_M/(N_2/He)_M$$
$$+ f_S/(N_2/He)_S \qquad (4)$$

$$f_A + f_M + f_S = 1 \qquad (5)$$

where f_A, f_M, and f_S are the air, mantle, and subducted hemipelagic sediment component fractions in each gas sample, respectively. The subscript "obs" indicates observed or measured values, while the subscripts "A," "M," and "S" denote the chosen endmember values for δ^{15}N or N_2/He. This model assumes that the magma is thoroughly degassed and the exsolved phase is sampled.

Table 6
Calculated air (A), mantle (M), and sediment (S) endmember contributions for Nicaraguan samples

Location	Sample ID	f_A	f_M	f_S	%S	$\delta^{15}N_{corr}$ (‰)	(L + S)/M[a]	f_A^c	f_M^c	f_S^c	%S[c]
Mombacho											
V. Mombacho[b]	Nic-15/1	0	0.54	0.46	45.7	0.49	11.2	0	0.30	0.70	70.4
Masaya											
Xiloá[b]	Nic-1	0	0.2	0.8	80.4	4.65	8.6	0	0.11	0.89	89.2
Momotombo											
Ormat power plant	Nic-14	0.025	0.39	0.58	59.7	2.16	19.9	0.01	0.22	0.77	77.9
V. Momotombo	Nic-2	0	0.2	0.8	80.5	4.66	17.3	0	0.11	0.89	89.2
V. Momotombo	Nic-3	0	0.04	0.96	96.1	6.53	17.3	0	0.02	0.98	97.8
Cerro Negro											
V. Cerro Negro[b]	Nic-24	0.11	0.25	0.64	72.0	3.64	20.0	0	0.10	0.90	90.2
Telica											
V. Telica	Nic-27	0.02	0.38	0.6	61.0	2.32	322	0.01	0.21	0.78	78.6

[a] Calculated component fractions of subducted pelagic limestone (L) and hemipelagic sediment (S) relative to upper mantle (M) for carbon and helium data, from Shaw et al. (2003).
[b] Samples Nic-1, Nic-15/1, and Nic-24 lie just outside but within error of the mixing curves and are projected back to the curves for calculations shown here. Nic-15/2 lies too far outside the curves for this to be reasonable, so no calculation results are shown.
[c] Alternate values calculated using a mantle endmember $\delta^{15}N$ value of −15‰ (see text).

The model also assumes that there are no nitrogen isotopic fractionation effects during degassing (Fischer et al., 2005). Calculated f_A, f_M, and f_S fractions for Nicaraguan gases are shown in Table 6, and the endmembers and calculated mixing lines are plotted with the Nicaragua data in Fig. 6a.

The component fractions in Table 6 are next used to calculate %S, or percent N_2 derived from sediment in a mantle-sediment binary mix, after air-correction of $\delta^{15}N$ values (after Fischer et al., 2002). The average fraction of N_2 derived from subducted sediment is 71% for Nicaragua. Component fraction and correction calculations can only be performed for data points lying within error of the mixing curves in Fig. 6a, which excludes sample Nic-15/2 from Mombacho. The sample does not fit our model, and it requires a subsurface process than can increase N_2/He without affecting $\delta^{15}N$. A low-helium source such as shallow organic matter is a possibility, but its nitrogen would have to have a negative $\delta^{15}N$ value. Alternatively, the chosen mantle endmember composition could be in error. Clor et al. (2005) have investigated this possibility by selecting −15‰ for the $\delta^{15}N$ value (Mohapatra and Murty, 2004) of the mantle. Fig. 6b and Table 6 show the results from using this endmember value. Sample 15/2 still lies outside the mixing curves because of changes in the mixing line curvature, so this cannot sufficiently explain the outlier. Further work on back-arc basin basaltic $\delta^{15}N$ values could further test the hypothesis that the mantle has a more extreme N isotope signature. Note that calculated %S values are significantly higher for all samples using this mantle endmember and average 85%.

5.3. Along-arc variations

Documented along-arc variations in subduction zone parameters in Central America allow us to investigate whether or not the proportions of N_2, He, and Ar, the nitrogen isotope systematics, and the CO_2/N_2 ratios are sensitive tracers for the processes that control volatile release from the slab. Shaw et al. (2003) showed that the CO_2/^{3}He values for gases from Nicaragua and Costa Rica are typical of arc settings (Table 4) and that there are no systematic variations in the relative contributions of carbonate and organic C along this segment of the arc. The overall contribution of slab-derived C relative to C originating from the mantle wedge, however, is significantly higher in Nicaragua than in Costa Rica (Shaw et al., 2003). The enhanced slab contribution in Nicaragua agrees with earlier findings (i.e. ^{10}Be (Morris et al., 1990), B/La (Leeman et al., 1994), Ba/La (Carr et al., 1990; Patino et al., 2000)). Fischer et al. (2002) and Zimmer et al. (2004) showed that the slab-derived contribution of N_2 to arc magmas in most of Costa Rica is <50% of the total, reflecting offscraping of N-rich hemipelagic sediments beneath Costa Rica. Along-arc variations in N_2 and CO_2 sources have also been observed by Snyder et al. (2001) and Snyder et al. (2003) in Central America and by Clor et al. (2005) and Jaffe et al. (2004) in the Sangihe arc, Indonesia and have been explained by crustal contributions, variations in subducted sediment composition, forearc devolatilization, and offscraping of oceanic sediments prior to subduction.

The model of Carr et al. (1990), described in Section 2, relates the sedimentary fluid contributions to Central American lavas to changes in slab dip. Leeman et al. (1994) further explain the low sediment signature in Costa Rican lavas with a scenario of sediment offscraping in the early stages of subduction, which does not occur beneath Nicaragua. In addition to supporting the scenario described by Carr et al. (1990) and Leeman et al. (1994), Shaw et al. (2003) suggest an alternative explanation for the variations in which the Nicaraguan thermal regime is characterized by a colder slab at depth due to steeper sub-
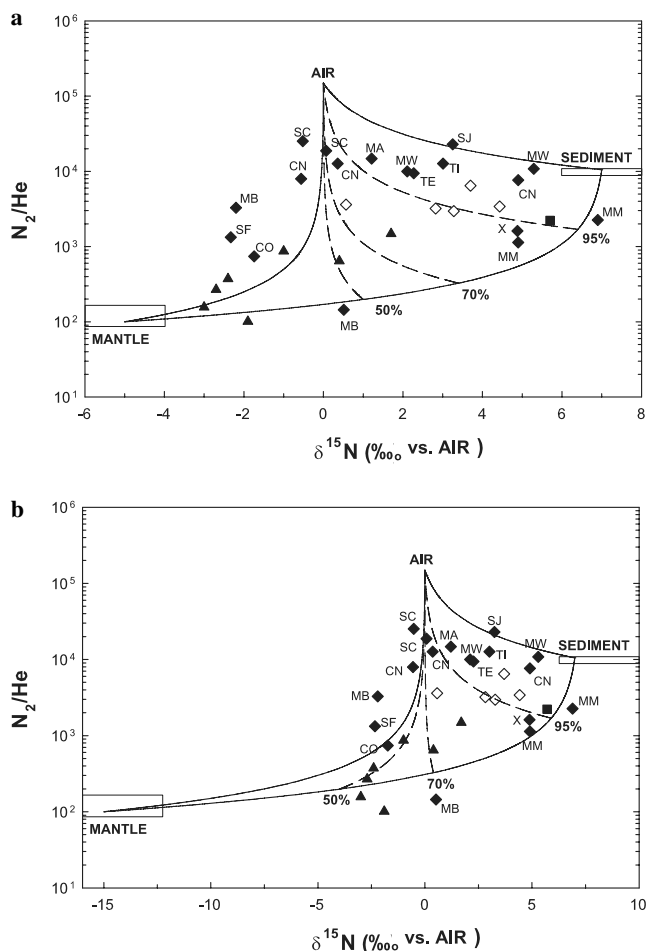
Fig. 6. $\delta^{15}N$ vs. N_2/He diagrams for Nicaraguan geothermal and volcanic gases. Calculations for mixing lines between air, mantle, and sediment are after Sano et al. (2001) and Fischer et al. (2002) and are described in the text. Triangles, Costa Rican gases (Fischer et al., 2002; Zimmer et al., 2004); square, Fuego, Guatemala (Fischer et al., 2002); open diamonds, Nicaragua (Snyder et al., 2003); filled diamonds, Nicaragua (this study). (a) Mixing lines calculated using a mantle $\delta^{15}N = -5‰$. (b) Mixing lines calculated using a mantle $\delta^{15}N = -15‰$. Symbols after Figs. 2 and 4.

duction. This in turn causes the slab to retain many of its volatile elements during the initial stages of subduction, which are then released in large quantities beneath the arc.

In order to evaluate whether subduction forcing functions influence the release of volatiles from the slab, we investigate along-arc variations in the volatile emissions using Fig. 7. This figure illustrates how samples from central and northern Nicaragua (Masaya, Momotombo, Cerro Negro, and Telica) show average $\delta^{15}N$ values ranging from 2.3‰ to 4.9‰, whereas Mombacho (the southernmost sample) has a $\delta^{15}N$ value of −2.2‰ (Table 4). Sediment-derived N based on N_2/He and N isotope ratios of central and northern Nicaragua samples is in excess of 50% (Table 6).

Gases from the northern Nicaraguan volcanoes (Cerro Negro and Telica) also have relatively high N_2 exc. abundances (∼150 to ∼185 mmol/mol). Central Nicaraguan gases (Masaya and Momotombo) have lower N_2 exc. abun-

dances (8.0 to ∼100 mmol/mol) and Mombacho has a N_2 exc. value of only 2.1 mmol/mol. Along-arc variations are also observed in the CO_2/N_2 exc. ratios. Northern Nicaraguan (Cerro Negro and Telica) CO_2/N_2 exc. ratios are <6; central Nicaraguan samples have CO_2/N_2 exc. ratios of ∼40 and Mombacho gases show an average ratio of ∼600 (Table 4). The majority of the Nicaraguan samples have significantly lower CO_2/N_2 exc. ratios than in other locales. CO_2/N_2 exc. ratios in volcanic arc gases overlap with but are generally lower than MORB (100–10,000; Marty and Zimmermann, 1999), suggesting that N in the emitted gases derives mainly from subducted materials while CO_2 comes from both the subducted slab and the mantle wedge (Fischer and Marty, 2005). We note that the N_2–He–CO_2 and N isotope systematics of Nicaragua gases are similar to the samples from Guatemala to the north (Fischer et al., 2002) and distinctly different from samples collected in Costa Rica to the south (Fig. 7; Fischer et al., 2002; Zimmer et al., 2004).

Sadofsky and Bebout (2004) calculate a total sedimentary input CO_2/N_2 ratio of 216, Li and Bebout (2005) find a ratio of 269 at the Central America Trench, and Marty and Zimmermann (1999) measure an average CO_2/N_2 mantle ratio from MORB glasses of 1070 ± 448. Thus, mixing between mantle and subducted sediment cannot produce the low CO_2/N_2 exc. ratios observed in central and northern Nicaragua and Guatemala. The low ratios in this section of the arc could result from preferential return of carbon to the mantle over nitrogen, whereas to the south (Mombacho and Costa Rican volcanoes) nitrogen is lost due to offscraping of the hemipelagic sediment layer or forearc devolatilization. The input flux ratio of oxidized C:organic C:N is 115:11:1 along the Central American margin (Li and Bebout, 2005). The ratio of oxidized C to organic C (10.5) corresponds closely to the L/S ratio measured in the gas discharges along the arc (9.6–11.1; Shaw et al., 2003), suggesting that there is no fractionation of oxidized and organic C during subduction, release from the slab, and transport through the mantle wedge. The organic C/N ratio of subducted sediments (11) is similar to the C/N ratios in the majority of Nicaraguan gases (4.2 to ∼40; Table 4). Because Shaw et al. (2003) did not observe systematic variations in L/S ratios from central to northern Nicaragua, variable contributions of oxidized and organic C to arc magmas are an unlikely cause for observed changes in CO_2/N_2 exc.. We therefore favor the idea that variable amounts of N released from the slab result in changes in the CO_2/N_2 exc. of the gases. Higher CO_2/N_2 exc. gas ratios than input organic C/N (11) suggest loss of N either by devolatilization in the forearc or by subduction past the zone of arc magma generation beneath southern and central Nicaragua localities. On the other hand, ratios below the organic C/N value of 11, as observed in northern Nicaragua, suggest that N is added from the subducted oceanic basement. Li and Bebout (2005) find that at least as much nitrogen could be released from the subducting basement as they calculate for the down-going sediment column.
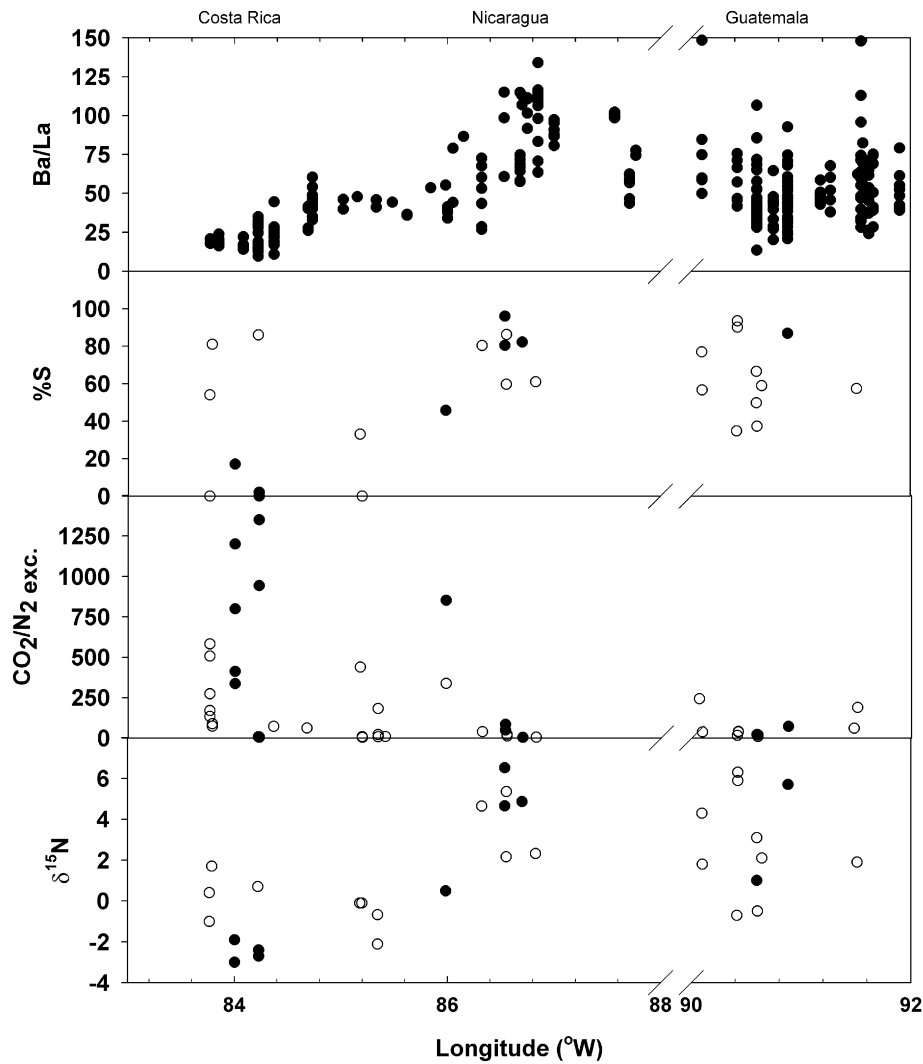
Fig. 7. Diagram showing $\delta^{15}N$, $CO_2/N_{2 \, exc.}$, %S, and Ba/La vs. latitude for the CAVA. Nicaragua data are from this study. Guatemala and Costa Rica data are from Fischer et al. (2002) and Zimmer et al. (2004). Selected Ba/La data are from Patino et al. (2000) and Carr et al. (2003). Open symbols represent geothermal gases and filled symbols are volcanic gases.

Lower $CO_2/N_{2 \, exc.}$ ratios in northern Nicaragua could be the result of preferential recycling of C into the deep mantle over nitrogen. Recycling of carbon into the mantle has been proposed based on mass balance considerations along the Central American Arc (Snyder et al., 2001; Shaw et al., 2003) and metamorphic phase relationships in subducted sediments and oceanic crust (Kerrick and Connolly, 2001a,b). If, however, preferential recycling of C were the case in only northern Nicaragua, then the amount of slab-derived C relative to mantle wedge C would be lower in the northern than in the central and southern parts of Nicaragua, and this is not observed (Shaw et al., 2003).

In summary, a scenario where steep subduction creates a colder slab at depth and allows volatiles to be retained (Shaw et al., 2003) applies to localities of central and northern Nicaragua, where the percentage of sediment contribution is highest (based on N-isotope systematics) and where the $CO_2/N_{2 \, exc.}$ ratios are similar to the ratio of organic C/N measured in subducted sediments. In southern

Nicaragua (Mombacho) a hotter and shallower slab results in the preferential loss of N over C in the forearc either by devolatilization or by sediment offscraping.

5.4. Nitrogen flux and mass balance

In order to assess whether nitrogen is efficiently cycled through the Central American subduction zone, as proposed by Fischer et al. (2002), or whether it is efficiently recycled into the deep mantle (Sadofsky and Bebout, 2004), we must quantify the N input and output flux through arc volcanism. Hilton et al. (2002) calculated a hemipelagic sediment-derived N input at the trench of 2.3×10^8 mol/a for the entire CAVA (corresponds to 6.4×10^7 mol/a for Nicaragua), and new data for N concentrations in the upper part of sediment cores (Li et al., 2003; Sadofsky and Bebout, 2004) give a slightly higher N input rate of 7.1×10^8 mol/a (2.0×10^8 mol/a for Nicaragua). Li and Bebout (2005) find a sediment-derived N input

of 9.3×10^8 mol N/a for the CAVA (2.6×10^8 mol/a for Nicaragua).

We estimate nitrogen fluxes from the passively degassing Nicaraguan volcanic front by three different methods. In the first method, estimated global ^{3}He fluxes (1000 mol/a) are scaled first to arcs (92.4 mol/a) and then to Central America (3.1 mol/a) using relative trench lengths (after Hilton et al., 2002; Shaw et al., 2003), and finally to Nicaragua with relative volcanic front lengths (Von Huene and Scholl, 1991; Protti et al., 1995). The global trench length is estimated at ~43,400 km, the CAVA trench length is ~1450 km, the CAVA volcanic front length is ~1060, and Nicaragua's volcanic front length is ~300 km. The resulting ^{3}He flux for Nicaragua of 0.86 mol/a was then multiplied by the average $N_{2\ exc.}/^3$He ratio for the uncontaminated volcanic and geothermal gases in this study (6×10^8). The $N_{2\ exc.}$ flux was multiplied by two (there are two N atoms for every N_2 molecule) to derive a N flux of 1.1×10^9 mol/a for Nicaragua.

In the second method we use the SO_2 flux measured at Nicaraguan volcanoes. This flux was calculated applying the method of Brantley and Koepenick (1995), in which the total flux for a region is evaluated from known fluxes for individual volcanoes with a power law function (after Hilton et al., 2002). Time averaged SO_2 flux data for four Nicaraguan volcanoes were available from Andres and Kasgnoc (1998), and with the power law function yielded a Nicaraguan SO_2 flux of 9.7×10^9 mol/a (the sum of the SO_2 fluxes from the four Nicaraguan volcanoes is 8.8×10^9 mol/a). By comparison, using the same techniques, Costa Rican SO_2 flux is equal to only 1.09×10^9 mol/a (Zimmer et al., 2004), total Central American flux is 21.3×10^9 mol/a (Hilton et al., 2002), and global flux is 315.7×10^9 mol/a. The average $S_t/N_{2\ exc.}$ ratio for Nicaragua was calculated using volcanic samples only, since hydrothermal processes strongly affect sulfur concentrations (Giggenbach, 1996). Samples from three Nicaraguan volcanic centers, Cerro Negro, Mombacho, and Momotombo, are considered to be of volcanic origin (see Section 4.1). Averages of data from these three centers are used to determine a $S_t/N_{2\ exc.}$ ratio for Nicaragua of 19.2. This gives a N flux of 9.7×10^8 mol/a.

The third method employs CO_2 fluxes, which were in turn calculated from ^{3}He and SO_2 fluxes. Shaw et al. (2003) used ^{3}He fluxes to determine the Central American CO_2 flux, which we have scaled to Nicaragua using relative volcanic front lengths. This gives a CO_2 flux of 2×10^{10} mol/a. We also determined a CO_2 flux from the SO_2 flux calculated above, using the average CO_2/S_t ratio from the high temperature, volcanic samples from Cerro Negro, Mombacho, and Momotombo (13.0). That CO_2 flux equals 1.2×10^{11} mol/a. The $CO_2/N_{2\ exc.}$ ratio used for these calculations is the average from all of the uncontaminated, robust Nicaraguan gas samples (137.5), and the resulting N fluxes are equal to 2.9×10^8 mol/a (from ^{3}He flux) and 1.8×10^9 mol/a (from SO_2 flux).

The minimum and maximum N fluxes calculated above differ by a factor of 6.2. Sediment-derived N flux is calculated using the average %S of 71%, and ranges from 2.1×10^8 to 1.3×10^9 mol/a for Nicaragua. Using the average value of 85 %S calculated with $\delta^{15}N = -15‰$ for the mantle endmember gives a sediment-derived N flux of 2.5×10^8 to 1.5×10^9 mol/a for Nicaragua. Sediment-derived CAVA N flux is then extrapolated using the volcanic front lengths described above (ranging from 7.4×10^8 to 4.6×10^9 mol/a), and global arc sediment-derived N flux is calculated using relative trench lengths (1.8×10^{11} mol/a). Calculated results are tabulated in Table 7.

Our Nicaraguan N fluxes range from 2.9×10^8 to 1.8×10^9. The calculated CAVA and global arc N fluxes range from within an order of magnitude to over an order of magnitude higher than previous estimates from Sano et al. (2001) and Fischer et al. (2002), while our values bracket a flux estimate from Hilton et al. (2002).

All of the above input fluxes for the CAVA (2.3 to 9.3×10^8 mol/year) lie at the low end of our calculated outputs (7.4 to 46×10^8 mol/year). However, Li and Bebout (2005) also calculate a possible additional altered ocean crust input of 5.3×10^8 to 5.3×10^9 mol N/a for Central America, resulting in a total N input of 1.5×10^9 to 6.2×10^{10} mol/a for the entire arc, and 5.5×10^8 to 2.3×10^9 mol/a for Nicaragua. This amount is more than sufficient to balance our highest estimates of N output for the entire CAVA (7.4×10^8 to 4.6×10^9 mol/year) and for Nicaragua (2.9×10^8 to 1.8×10^9 mol/year). Bebout (1995) and Sadofsky and Bebout (2004) have shown that alteration in ocean sediments leads to fractionation and heavier nitrogen isotope values in the remaining materials. If this occurs in ocean basalts as well, altered ocean basement could indeed provide an additional source of subducted ^{15}N-rich nitrogen, though it is difficult to estimate altered ocean crust δ^{15}N. Further work on nitrogen fractionation during alteration of ocean basalts could provide insight into the importance of this largely unconsidered reservoir for nitrogen subduction budgets. N concentrations in oceanic crust are variable and not well constrained, but could conservatively range from 5 to 50 ppm (Li and Bebout, 2005). To calculate their altered ocean crust input fluxes, Li and Bebout (2005) use a crustal thickness of 5 km.

If altered ocean crust is considered, our average Central American N output of 2.7×10^9 mol/a accounts for 41.9% of the subducted nitrogen, and the remainder is either subducted into the deep mantle or devolatilized in the forarc. On the other hand, if altered crust is not a significant source of subducted N for Central American volcanic and geothermal gases, approximately 100% of the subducted nitrogen is emitted from volcanic front volcanoes in Nicaragua. In this case, little or none of the subducted nitrogen is being recycled back into the mantle beyond the zone of arc magma generation beneath Nicaragua.

Table 7
Calculated nitrogen fluxes for the Nicaraguan volcanic front, in 10^8 mol/a

	Nic N flux	Sediment-derived N flux (%S = 71%)			(%S = 85%)
		Nicaragua	CAVA	Global arcs	Nicaragua
N flux (this study)					
Calculated from ^{3}He	11	7.8	28		9.4
Calculated from SO_2	9.7	6.9	25		8.2
Calculated from CO_2,^{3}He	2.9	2.1	7.4		2.5
Calculated from CO_2, SO_2	18	12.8	46		15.3
Averages	10.4	7.4	27	1800	8.8
Previous work: N flux					
Sano et al. (2001)			0.19	13	
Fischer et al. (2002)			2.9	200	
Hilton et al. (2002)			17	320	
Snyder et al. (2003):					
Minimum...				54	
Maximum...				110	
N inputs					
Fischer et al. (2002)			2.3		
Hilton et al. (2002)			5.5	69	
Li et al. (2003)			7.1		
Snyder et al. (2003)				92	
Zimmer et al. (2004):					
Minimum...			0.49		
Maximum...			1.05		
Li and Bebout (2005):					
Subducted sediment...		9.3			
+ Altered ocean crust [N] = 5 ppm...	14				
= 50 ppm...	62				

6. Conclusions

From the analyses of 26 volatile samples collected in the Nicaraguan segment of the Central American Volcanic Arc, we draw the following conclusions:

(1) Geographic variability in gas chemistry exists along the volcanic front, whereby a larger sediment fingerprint is observed in gases from northwestern Nicaragua than elsewhere in the segment. Evidence for the subducting sediment contribution to the gases is seen in the form of δ^{15}N values approaching +7‰ and N_2/He ratios nearing 10,500. Higher $CO_2/N_{2\ exc.}$ ratios and lower δ^{15}N in the south and in Costa Rica suggest a high mantle input of N beneath the arc, while progressively lower $CO_2/N_{2\ exc.}$ ratios to the north indicate preferential nitrogen release over carbon from subducted sediments and/or contributions from altered oceanic crust. These variations reveal an affinity with Guatemalan gas chemistry in the northwest and a similarity to Costa Rican chemistry in southeastern Nicaragua. Calculated sediment contributions to the gases average 71% if the mantle has δ^{15}N of −5‰ (contributions range from 45.7% to 96.1% for Nicaragua) and 85% for a mantle with δ^{15}N of −15‰.

(2) Air-corrected, sediment-derived nitrogen flux in Nicaragua was determined to be 7.8×10^8 mol/a using ^{3}He flux, 6.9×10^8 mol/a using SO_2 flux, and 2.1×10^8 and 1.3×10^9 mol/a using CO_2 fluxes calculated from ^{3}He and SO_2, respectively, with a mantle δ^{15}N of −5‰. The average sediment-derived N flux calculated is 7.4×10^8 mol/a for Nicaragua and 2.7×10^9 mol/a for all of Central America. These are higher than previously calculated fluxes, due to the uniquely high sediment-derived nitrogen content of Nicaraguan gases (71 %S). Using a mantle δ^{15}N value of −15‰ and a resulting sediment-derived N content of 85%, the same sediment-derived fluxes are 9.4×10^8, 8.2×10^8, 2.5×10^8, and 1.5×10^9 mol/a, respectively, with an average N flux of 8.8×10^8 mol/a. These averages are higher than estimated nitrogen inputs at the trench, but are within an order of magnitude of those values. The input of additional nitrogen sources at the trench, such as altered oceanic basement, could provide enough nitrogen to account for this difference. The estimates indicate that most or all of the subducted sedimentary nitrogen is being returned to the surface through volcanism in Nicaragua.

(3) If alteration of oceanic basalts causes fractionation to heavier nitrogen isotope values, subducted oceanic basement could serve as a source of isotopically heavy nitrogen in geothermal fluids. This is a largely unconsidered reservoir in nitrogen subduction budgets. If it is an important reservoir of nitrogen in volcanic arcs, significant quantities of nitrogen could be

returned to the mantle during subduction. However, if altered crust does not act as a major reservoir for subducting nitrogen, we estimate that all of the nitrogen subducted off Nicaragua is emitted from volcanic and geothermal sources along the volcanic front.

Acknowledgments

Associate editor: Bernard Marty

Appendix A. Supplementary data

Supplementary data associated with this article can be found, in the online version, at doi:10.1016/j.gca.2006.07.024.

References

Allard, P., 1983. The origin of hydrogen, carbon, sulphur, nitrogen and rare gases in volcanic exhalations: Evidence from isotope geochemistry. In: Tazieff, H., Sabroux, J.C. (Eds.), *Forecasting Volcanic Events*. Elsevier, Amsterdam.

Andres, R.J., Kasgnoc, A.D., 1998. A time-averaged inventory of subaerial volcanic sulfur emissions. *J. Geophys. Res.* **13** (25), 25,251–25,261.

Ballentine, C.J., Burgess, R., Marty, B., 2002. Tracing fluid origin, transport and interaction in the crust. In: Porcelli, D., Ballentine, C.J., Wieler, R. (Eds.), *Noble Gases in Geochemistry and Cosmochemistry*. Min. Soc. Am., Washington, DC, pp. 539–614.

Beaty, R.D., Kerber, J.D., 1993. *Concepts, Instrumentation and Techniques in Atomic Absorption Spectrophotometry*. Perkin-Elmer, Norwalk, CT.

Bebout, G.E., 1995. The impact of subduction-zone metamorphism on mantle-ocean chemical cycling. *Chem. Geol.* **126**, 191–218.

Bebout, G.E., Fogel, M.L., 1992. Nitrogen-isotope compositions of metasedimentary rocks in the Catalina Schist, California: implications for metamorphic devolitilization history. *Geochim. Cosmochim. Acta* **56**, 2839–2849.

Boyd, S.R., Pillinger, C.T., 1994. A preliminary study of $^{15}N/^{14}N$ in octahedral growth form diamonds. *Chem. Geol.* **116**, 43–59.

Brantley, S.L., Koepenick, K.W., 1995. Measured carbon dioxide emissions from Oldoinyo Lengai and the skewed distribution of passive volcanic fluxes. *Geology* **23**, 933–936.

Carr, M.J., 1984. Symmetrical and segmented variation of physical and geochemical characteristics of the Central American volcanic front. *J. Volcanol. Geotherm. Res.* **20**, 231–252.

Carr, M.J., Feigenson, M.D., Bennett, E.A., 1990. Incompatible element and isotopic evidence for tectonic control of source mixing and melt extraction along the Central American arc. *Contrib. Mineral. Petrol.* **105**, 369–380.

Carr, M.J., Feigenson, M.D., Patino, L.C., Walker, J.A., 2003. Volcanism and Geochemistry in Central America: Progress and Problems. In Inside the Subduction Factory, *Geophys. Mon.* **138**, 153–179.

Cartigny, P., Harris, J.W., Javoy, M., 1998. Subduction-related diamonds? The evidence for a mantle-derived origin from coupled δ^{13}C-δ^{15}N determinations. *Chem. Geol.* **147**, 147–159.

Chiodini, G., Cioni, R., Frullani, A., Giudi, M., Marini, L., Prati, F., Raco, B., 1996. Fluid geochemistry of Monserrat Island, W. Indies. *Bull. Volcanol.* **58**, 380–392.

Clor, L.E., Fischer, T.P., Hilton, D.R., Sharp, Z.D., Hartono, U., 2005. Volatile and N isotope chemistry of the Molucca Sea collision zone: Tracing source components along the Sangihe Arc, Indonesia. *Geochem. Geophys. Geosys.* **6**. doi:10.1029/2004GC000825.

Corti, G., Carminati, E., Mazzarini, F., Garcia, M.O., 2005. Active strike-slip faulting in El Salvador, Central America. *Geology* **33**, 989–992.

Craig, H., 1961. Isotopic variations in meteoric waters. *Science* **133**, 1702–1703.

Criss, R.E., 1999. *Principles of Stable Isotope Distribution*. Oxford University Press, New York.

Crovetto, R., 1996. In: Scharlin, P. (Ed.), *Solubility Data Series*, vol. 62. Pergamon Press.

D'Amore, F., Panichi, C., 1980. Evaluation of deep temperatures of hydrothermal systems by a new gas geothermometer. *Geochim. Cosmochim. Acta* **44**, 549–556.

DeMets, C., Gordon, R.G., Argus, D.F., Stein, S., 1990. Current plate motions. *Geophys. J. Int.* **101**, 425–478.

Dixon, J.E., Stolper, E.M., Holloway, J.R., 1995. An experimental study of water and carbon dioxide solubilities in mid-ocean ridge basaltic liquids; part I: calibration and stability models. *J. Petrol.* **36**, 1607–1631.

Eiler, J.M., Carr, M.J., Reagan, M., Stolper, E., 2005. Oxygen isotope constraints on the sources of Central American arc lavas. *Geochem. Geophys. Geosys.* **6**. doi:10.1029/2004GC000804.

Fischer, T.P., Marty, B., 2005. Volatiles in the sub-arc mantle: insights from volcanic and hydrothermal gas emissions. *J. Volcanol. Geotherm. Res.* **140**, 205–216.

Fischer, T.P., Giggenbach, W.F., Sano, Y., Williams, S.N., 1998. Fluxes and sources of volatiles discharged from Kudryavy, a subduction zone volcano, Kurile Islands. *Earth Planet. Sci. Lett.* **160**, 81–96.

Fischer, T.P., Hilton, D.R., Zimmer, M.M., Shaw, A.S., Sharp, Z.D., Walker, J.A., 2002. Subduction and recycling of nitrogen along the Central American Margin. *Science* **297**, 1154–1157.

Fischer, T.P., Takahata, N., Sano, Y., Sumino, H., Hilton, D.R., 2005. Nitrogen isotopes of the mantle: insights from mineral separates. *Geophys. Res. Lett.* **32**, 2005GL022792.

Giggenbach, W.F., 1992. The composition of gases in geothermal and volcanic systems as a function of tectonic setting. In: Kharaka, Y.K., Maest, A. (Eds.), *Water–Rock Interaction*. Balkema, Rotterdam, pp. 873–877.

Giggenbach, W.F., 1995. Composition of fluids in geothermal systems of the Taupo Volcanic Zone, New Zealand, as a function of source magma. In: Chudaev K.A. (Ed.), *Water–rock Interaction*, **vol. 8**, pp. 9–12.

Giggenbach, W.F., 1996. Chemical composition of volcanic gases. In: Scarpa, R., Tilling, R. (Eds.), *Monitoring and Mitigation of Volcanic Hazards*. Springer, pp. 221–256.

Giggenbach, W.F., Goguel, R.L., 1989. Methods for the collection and analysis of geothermal and volcanic water and gas samples. *Dept. Scient. Indust. Res.*, N.Z., #CD 2387 (report).

Giggenbach, W.F., Soto, R.C., 1992. Isotopic and chemical composition of water and steam discharges from volcanic-magmatic-hydrothermal systems of the Guanacaste Geothermal Province, Costa Rica. *Appl. Geochem.* **7**, 309–332.

Giggenbach, W.F., Garcia, N., Londoño, A., Rodriguez, L., Rojas, N., Calvache, M.L., 1990. The chemistry of fumarolic vapor and thermal-spring discharges from the Nevado del Ruiz volcanic-magmatic-hydrothermal system, Columbia. *J. Volcanol. Geotherm. Res.* **42**, 13–39.

Goff, F., McMurtry, G.M., 2000. Tritium and stable isotopes of magmatic waters. *J. Volcanol. Geotherm. Res.* **97**, 347–396.

Hilton, D.R., Hammerschmidt, K., Teufel, S., Friedrichsen, H., 1993. Helium isotope characteristics of Andean geothermal fluids and lavas. *Earth Planet. Sci. Lett.* **120**, 265–282.

Hilton, D.R., Fischer, T.P., Marty, B., 2002. Noble gases and volatile recycling at subduction zones. In: Porcelli, D., Ballentine, C.J., Wieler, R. (Eds.), *Noble Gases in Geochemistry and Cosmochemistry*. Min. Soc. Am., Washington, DC, pp. 319–370.

Jaffe, L.A., Hilton, D.R., Fischer, T.P., Hartono, U., 2004. Tracing magma sources in an arc-arc collision zone: Helium and carbon isotope and relative abundance systematics of the Sangihe Arc, Indonesia. *Geochem. Geophys. Geosys.* **5**. doi:10.1029/2003GC000660.

Jambon, A., Weber, H., Braun, O., 1986. Solubility of He Ne, Ar, Kr and Xe in a basalt melt in the range 1250–1600 °C: geochemical implications. *Geochim. Cosmochim. Acta* **50**, 401–408.

Kerrick, D.M., Connolly, J.A.D., 2001a. Metamorphic devolatilization of subducted marine sediments and the transport of volatiles into the Earth's mantle. *Nature* **411**, 293–296.

Kerrick, D.M., Connolly, J.A.D., 2001b. Metamorphic devolatilization of subducted oceanic metabasalts: implications for seismicity, arc magmatism and volatile recycling. *Earth Planet. Sci. Lett.* **189**, 19–29.

Kienast, M., 2000. Unchanged nitrogen isotopic composition of organic matter in the South China Sea during the last climatic cycle: global implications. *Paleoceanography* **15**, 244–253.

Kita, I., Nitta, K., Nagao, K., Taguchi, S., Koga, A., 1993. Difference in N_2/Ar ratio of magmatic gases from Northeast and Southwest Japan: New evidence for different states of plate subduction. *Geology* **21**, 391–394.

Leeman, W.P., Carr, M.J., 1995. Geochemical constrains on subduction processes in the Central American Volcanic Arc: Implications of bororn geochemistry. *Geol. Soc. Am. Spec. paper* **295**, 57–73.

Leeman, W.P., Carr, M.J., Morris, J.D., 1994. Boron geochemistry of the Central American volcanic arc: constraints on the genesis of subduction-related magmas. *Geochim. Cosmochim. Acta* **58**, 149–168.

Li, L., Bebout, G.E., 2005. Carbon and nitrogen geochemistry of sediments in the Central American convergent margin: Insights regarding paleoproductivity and carbon and nitrogen subduction fluxes. *J. Geophys. Res.* **110**. doi:10.1029/2004JB003276.

Li, L., Sadofsky, S.J., Bebout, G.E., 2003. Carbon and nitrogen input fluxes in subduction sediments at the Izu-Bonin and Central America convergent margins. *Eos Trans. Am. Geophys. Union* **84**, Fall Meet. Suppl. #T32A-0908 (abstr.).

Libourel, G., Marty, B., Humbert, F., 2003. Nitrogen solubility in basaltic melt: part I, effect of oxygen fugacity. *Geochim. Cosmochim. Acta* **67**, 4123–4135.

Lide, D.R., 1990. *The CRC Handbook of Chemistry and Physics*, 71st ed. CRC Press, Boca Raton, FL.

Lux, G.E., 1987. The behavior of noble gases in silicate liquids: solution, diffusion, bubbles and surface effects, with applications to natural samples. *Geochim. Cosmochim. Acta* **51**, 1549–1560.

Mariner, R.H., Evans, W.C., Presser, T.S., White, L.D., 2003. Excess nitrogen in selected thermal and mineral springs of the Cascade Range in northern California, Oregon, and Washington: sedimentary or volcanic in origin?. *J. Volcanol. Geotherm. Res.* **121** 99–114.

Marty, B., 1995. Nitrogen content of the mantle inferred from N_2-Ar correlation in oceanic basalts. *Nature* **377**, 326–329.

Marty, B., Dauphas, N., 2003. The nitrogen record of crust-mantle interaction and mantle convection from Archean to present. *Earth Planet. Sci. Lett.* **206**, 397–410.

Marty, B., Humbert, F., 1997. Nitrogen and argon isotopes in oceanic basalts. *Earth Planet. Sci. Lett.* **152**, 101–112.

Marty, B., Zimmermann, L., 1999. Volatiles (He, N, C, Ar) in mid-ocean ridge basalts: assessment of shallow-level fractionation and characterization of source composition. *Geochim. Cosmochim. Acta* **63**, 3619–3633.

Matsuo, S., Suzuki, M., Mizutani, Y., 1978. Nitrogen to argon ratio in volcanic gases. In: Alexander, E.C., Jr.Jr., Ozima, M. (Eds.), *Terrestrial Rare Gases*. Japan Science Society Press, pp. 17–25.

Menyailov, I.A., Nikitina, L.P., Shapar, V.N., Pilipenko, V.P., 1986. Temperature increase and chemical change of fumarolic gases at Momotombo Volcano, Nicaragua, in 1982-1985: are these indicators of a possible eruption? *J. Geophys. Res.* **B91**, 12,199–12,214.

Minster, J.B., Jordan, T.H., 1978. Present-day plate motions. *J. Geophys. Res.* **A83**, 5331–5354.

Mohapatra, R.K., Murty, S.V.S., 2004. Nitrogen isotopic composition of the MORB mantle: a reevaluation. *Geochem. Geophys. Geosys.* **5**. doi:10.1029/2003GC000612.

Morris, J.D., Leeman, W.P., Tera, F., 1990. The subducted component in island arc lavas: constraints from Be isotopes and B-Be systematics. *Nature* **344**, 31–36.

Ozima, M., Podosek, F.A., 2002. *Noble Gas Geochemistry*, second ed. Cambridge University Press, Cambridge.

Patino, L.C., Carr, M.J., Feigenson, M.D., 2000. Local and regional variations in Central American arc lavas controlled by variations in subducted sediment input. *Contrib. Mineral. Petrol.* **138**, 265–283.

Peters, K.E., Sweeney, R.E., Kaplan, I.R., 1978. Correlation of carbon and nitrogen stable isotope ratios in sedimentary organic matter. *Limnol. Oceanogr.* **23**, 598–604.

Protti, M., Güendel, F., McNally, K., 1995. Correlation between the age of the subducting Cocos plate and the geometry of the Wadati-Benioff zone under Nicaragua and Costa Rica. *Geol. Soc. Spec. Pub.* **295**, 309–326.

Sadofsky, S.J., Bebout, G.E., 2004. Nitrogen geochemistry of subducting sediments: new results from the Izu-Bonin-Mariana margin and insights regarding global nitrogen subduction. *Geochem. Geophys. Geosys.* **5**. doi:10.1029/2003GC000543.

Sano, Y., Nishio, Y., Gamo, T., Jambon, A., Marty, B., 1998. Noble gas and carbon isotopes in Mariana Trough basalt glasses. *Appl. Geochem.* **13**, 441–449.

Sano, Y., Takahata, N., Nishio, Y., Fischer, T.P., Williams, S.N., 2001. Volcanic flux of nitrogen from the Earth. *Chem. Geol.* **171**, 263–271.

Sharp, Z.D., Atudorei, V., Durakiewicz, T., 2001. A rapid method for determination of hydrogen and oxygen isotope ratios from water and hydrous minerals. *Chem. Geol.* **178**, 197–210.

Shaw, A.M., Hilton, D.R., Fischer, T.P., Walker, J., Alvarado, G., 2003. Contrasting volatile systematics of Nicaragua and Costa Rica: Insights to C cycling through subduction zones using He–C relationships. *Earth Planet. Sci. Lett.* **214**, 499–513.

Smith, R.E., 1988. *Ion Chromatography applications*. CRC Press, Boca Raton, FL.

Snyder, G., Poreda, R., Hunt, A., Fehn, U., 2001. Regional variations in volatile composition: Isotopic evidence for carbonate recycling in the Central American volcanic arc. *Geochem. Geophys. Geosys.* **2**. doi:10.1029/2001GC000163.

Snyder, G., Poreda, R., Fehn, U., Hunt, A., 2003. Sources of nitrogen and methane in Central American geothermal settings: noble gas and ^{129}I evidence for crustal and magmatic volatile components. *Geochem. Geophys. Geosys.* **4**. doi:10.1029/2002GC000363.

Taran, Y., Fischer, T.P., Porovsky, B., Sano, Y., Armienta, M.A., Macias, J.L., 1998. Geochemistry of the volcano-hydrothermal system of El Chichón volcano, Chiapas, Mexico. *Bull. Volcanol.* **59**, 436–449.

Von Huene, R., Scholl, D.W., 1991. Observations at convergent margins concerning sediment subduction, subduction erosion, and the growth of continental crust. *Rev. Geophys.* **29**, 279–316.

Von Huene, R., Aubouin, J., Azema, J., Blackinton, G., Coulbourn, W.T., Cowan, D.S., Curiale, J.A., Dengo, C.A., Faas, R.W., Harrison, W.,

Hesse, R., Hussong, D.M., Laad, J.W., Muzylov, N., Shiki, T., Thompson, P.R., Westberg, J., Carter, J.A., 2004. Leg 67: The Deep Sea Drilling Project Mid-America Trench transect off Guatemala. *Geol. Soc. Am. Bull.* **91**, 1421–1432.

Zimmer, M.M., Fischer, T.P., Hilton, D.R., Alvarado, G.E., Sharp, Z.D., Walker, J.A., 2004. Nitrogen systematics and gas fluxes of subduction zones: Insights from Costa Rica arc volatiles. *Geochem. Geophys. Geosys.* **5**. doi:10.1029/2003GC000651.